Si Ming-Sing (Orcid ID: 0000-0002-1927-420X)

TITLE: Tissue-Specific Angiogenic and Invasive Properties of Human Neonatal Thymus and Bone MSCs: Role of SLIT3-ROBO1

RUNNING HEAD: Role of SLIT3-ROBO1 in MSCs

AUTHORS: Shuyun Wang,[1] Shan Huang,[1] Sean Johnson,[1] Vadim Rosin,[1] Jeffrey Lee,[1] Eric Colomb,[1] Russell Witt,[2] Alexander Jaworski,[3] Stephen J. Weiss,[4] Ming-Sing Si,[1]

AFFILIATIONS: [1]Department of Cardiac Surgery, Section of Pediatric Cardiovascular Surgery, University of Michigan, Ann Arbor, MI 48109, USA; [2]Department of General Surgery, Brigham and Women's Hospital, MA 02115, USA; [3]Department of Neuroscience, Brown University, Providence, RI 02912, USA; [4]Department of Internal Medicine, University of Michigan, Ann Arbor, MI 48109, USA.

AUTHOR CONTRIBUTIONS:
Shuyun Wang: Collection and assembly of data, data analysis and interpretation, and manuscript writing.
Shan Huang: Collection and assembly of data.
Sean Johnson: Collection and assembly of data.
Vadim Rosin: Collection and assembly of data and data analysis and interpretation.
Jeffrey Lee: Collection and assembly of data.
Eric Colomb: Collection and assembly of data.
Russell Witt: Collection and assembly of data.
Alexander Jaworski: Provision of study material and manuscript writing.
Stephen J. Weiss: Conceptin and design, data analysis and interpretation, manuscript writing, and final approval of manuscript.
Ming-Sing Si: Conception and design, financial support, provision of study materials, collection and assembly of data, data analysis and interpretation, manuscript writing, and final approval of manuscript.

CORRESPONDENCE INFORMATION:
Ming-Sing Si, MD
University of Michigan
C.S. Mott Children's Hospital
Department of Cardiac Surgery
Floor 11, Room 735
1540 E. Hospital Drive
Ann Arbor, Michigan 48109
mingsing@umich.edu

This is the author manuscript accepted for publication and has undergone full peer review but has not been through the copyediting, typesetting, pagination and proofreading process, which may lead to differences between this version and the Version of Record. Please cite this article as doi: 10.1002/sctm.12723

ACKNOWLEDGEMENTS: Research reported in this publication was partially supported by the National Heart, Lung, And Blood Institute of the National Institutes of Health under Award Number K08HL146351 The content is solely the responsibility of the authors and does not necessarily represent the official views of the National Institutes of Health. Other support for this work was from the University of Michigan Department of Cardiac Surgery, University of Michigan Frankel Cardiovascular Center, Faith's Angels, and the Children's Heart Foundation. Assistance from the University of Michigan DNA Microarray Core is acknowledged.

CONFLICTS OF INTEREST: The authors declared no potential conflict of interest.

KEY WORDS: Mesenchymal stem cells, SLIT3, ROBO1, cell motility, angiogenesis

Data Availability Statement: The data that support the findings of this study are available on request from the corresponding author.

ABSTRACT

While MSCs are being explored in numerous clinical trials as proangiogenic and proregenerative agents, the influence of tissue origin on the therapeutic qualities of these cells is poorly understood. Complicating the functional comparison of different types of MSCs are the confounding effects of donor age, genetic background, and health status of the donor. Leveraging a clinical setting where MSCs can be simultaneously isolated from discarded but healthy bone and thymus tissues from the same neonatal patients, thereby controlling for these confounding factors, we performed an *in vitro* and *in vivo* paired comparison of these cells. We found that both neonatal thymus (nt)MSCs and neonatal bone (nb)MSCs expressed different pericytic surface marker profiles. Further, ntMSCs were more potent in promoting angiogenesis *in vitro* and *in vivo* and they were also more motile and efficient at invading ECM *in vitro*. These functional differences were in part mediated by an increased ntMSC expression of SLIT3, a factor known to activate endothelial cells. Further, we discovered that SLIT3 stimulated MSC motility and fibrin gel invasion via ROBO1 in an autocrine fashion. Consistent with our findings in human MSCs, we found that SLIT3 and ROBO1 were expressed in the perivascular cells of the neonatal murine thymus gland and that global SLIT3 or ROBO1 deficiency resulted in decreased neonatal murine thymus gland vascular density. In conclusion, ntMSCs possess increased proangiogenic and invasive behaviors which are in part mediated by the paracrine and autocrine effects of SLIT3.

INTRODUCTION

Mesenchymal stem/stromal cells (MSCs) are located in the perivascular region, can be isolated from a variety of tissues, and are being evaluated as proangiogenic and proregenerative therapies in numerous clinical trials [1-8]. While endothelial cells have been recently recognized to possess tissue-specific properties, the influence of tissue origin on MSC therapeutic effects is poorly understood [9,10].

The ability of MSCs to migrate to damaged tissues to exert its proregenerative, antiinflammatory and proangiogenic effects also influences their therapeutic potential [11-14]. Infusion of MSCs into the venous circulation result in intravascular homing to injured areas, and homing over shorter distances through the tissue interstitium are also likely to occur in the setting of local injection [15,16]. Requisite for homing is the motile and tissue-invasive abilities of MSCs, and the influence of tissue origin on these characteristics is not known [17]. The secreted axon guidance molecule SLIT3 has been shown to be an endothelial cell (EC) stimulant [18] and has been associated with a bone marrow derived MSC line that is proangiogenic [19]; however, it is not known if this finding can be generalized to other MSC lines.

Knowing these tissue-specific properties of MSCs is important because they may have translational implications for MSC therapies [20]. However, comparing MSCs from different tissues is confounded by factors such as donor age, presence of systemic disease, and individual variability [21-27]. We have been able to simultaneously isolate MSCs from thymus and bone tissue from neonates undergoing cardiac surgery, thereby allowing for a paired comparison that controls for the above confounding factors [28,29]. These two tissues have disparate perivascular

mural cell embryological origin and different degrees of perivascular mural cell coverage of the vasculature [30-34]. Based on these differences, we hypothesized that MSCs from the thymus and bone would have different proangiogenic, motile, and invasive characteristics. Using both *in vitro* and *in vivo* assays, we evaluated this hypothesis and identified that SLIT3 contributes to the observed differences in these functional properties of MSCs.

MATERIALS AND METHODS

Cell Isolation and Culture

Isolation, culture, and characterization of the human ntMSCs and nbMSCs used in these studies were previously described [28,29] under a protocol that was approved by the University of Michigan Institutional Review Board. Furthermore, Human adult bone marrow-derived (ab)MSCs were obtained from Lonza (Basel, Switzerland) and ATCC (Manassas, VA, USA), and human umbilical vein endothelial cells (HUVECs) were obtained from Lonza. Unless specified otherwise, all experiments utilized cells from passages 3-9.

Pericytic Signature Analysis

Pericyte surface markers of ntMSCs and nbMSCs isolated from n=3 patients were characterized by flow cytometry using fluorochrome-conjugated anti-human CD140a, CD140b, CD146, and CD90 (BD Biosciences, San Jose, CA). The antibodies were incubated with MSCs for 60 minutes at room temperature followed by three washes. MSCs were then analyzed using

a MoFlo® Astrios™ flow cytometer (Beckman Coulter, Inc., Pasadena, CA, USA) using the appropriate isotype-matched and unstained controls.

We also measured the transcript expression of *TBX18*, recently determined to be expressed in the perivascular mural cells of mice vasculature [8], in human ntMSCs, nbMSCs, and abMSCs using qPCR (see below).

MSC Conditioned Medium Generation and HUVEC Tube Formation Assay

Ninety-six-well plates were coated with 60 µl Matrigel matrix (10 mg/mL, Corning, NY, USA) per well at 37°C for 30 to 60 minutes. HUVEC suspensions were prepared using the corresponding medium at a concentration of 1.5 x 10^5 /mL. Next, 100 µl (15,000) of cells were added to each well (5 wells per group) on top of the gelled Matrigel followed by the addition of 100 µl of MSC conditioned medium and then incubated at 37°C, 5% CO_2 for 4 to 16 hours. Once tube formation was observed, the plate was washed with HBSS, and the cells were labeled with Calcein AM (2 µM) (ThermoFisher Scientific, Waltham, MA, USA) for 30 min at 37°C in 5% CO_2 and were photographed using a fluorescent microscope. In subsequent experiments, a blocking anti-SLIT3 antibody (5 µg/mL, AF3629, R&D Systems, Minneapolis, MN, USA) was added to the ntMSC derived conditioned medium to neutralize the effects of SLIT3.

Boyden Chamber Assay

Mesenchymal stromal cell migration was measured using the Boyden chamber assay (Cell Biolabs, Inc., San Diego, CA, USA) in a 24-well format with 8 µm pore size according to the manufacturer's instructions. In brief, 5 x 10^4 cells in 300 µl serum-free medium were seeded in the upper compartment (the insert) and then allowed to migrate through the pores of the

membrane into the lower compartment. After an appropriate incubation time in a cell culture incubator, migratory cells on the bottom of the polycarbonate membrane were stained and quantified in a fluorescence plate reader.

In Vitro Spheroid Angiogenic Sprouting Assay

Spheroids comprised of 800 MSCs or 400 MSCs/400ECs were generated by hanging drop culture as previously described [29]. Spheroids were embedded in fibrin gel and allowed to sprout for 20 hours. Brightfield images were then acquired digitally and were analyzed using NeuronJ as previously described [29]. In some experiments, rhSLIT3 (12.5 μg/ml) (R&D Systems, Minneapolis, MN, USA) was added to the media just after spheroids were embedded in fibrin gel. In other experiments, *SLIT3* or *ROBO1* gene targeting in MSCs was performed using siRNA (Origene, Rockville, MD, USA). Knockdown of gene expression was confirmed by qPCR before use in experiments, and experiments were repeated with at least two different siRNAs.

qPCR

Differential gene was performed using qPCR. RNA from cells was extracted according to the manufacturer's instructions using the RNeasy Mini Kit (Qiagen, Hilden, Germany) and 1 μg of total RNA was reverse transcribed with qScript cDNA Synthesis Kit (Quantabio, Beverly, MA, USA). Quantitative polymerase chain reactions were carried out with PerfeCTa SYBR Green supermix (Quantabio) and the Applied Biosystems (Foster City, CA USA), QuantStudio 5 Real-Time PCR System. Data were analyzed using the $2^{-\Delta\Delta C_T}$ method. The genes and primers used for this study are listed in Supplementary Table S1.

In Vivo Angiogenesis Assay

The care of animals was in accordance with institutional guidelines. Constructs (n=5/group) containing 2 million cells (HUVECs, MSCs, and HUVECs/MSCs at a 1:1 ratio) or no cells (control group) were made in 48-well plates with 200 µl of fibronectin and collagen hydrogel. Subject-matched ntMSCs and nbMSCs and unrelated abMSCs were utilized. Constructs were implanted subcutaneously in the dorsal region of NOD/SCID mice. Constructs were explanted 14 days after implantation for histological studies and CD31 immunohistochemistry (IHC) as previously described [29].

Microarray

Global gene expression from neonate-matched nbMSCs and ntMSCs was performed to gain further insight into the differences in their proangiogenic abilities. Total RNA was isolated from MSCs grown under standard conditions and then labeled and hybridized to Human Gene ST 2.1 human cDNA microarrays (Affymetrix, Santa Clara, CA, USA). Five biological replicates (individual neonates) were analyzed by the University of Michigan Microarray Core. Human Gene ST 2.1 human cDNA microarrays (Affymetrix) were used to compare ntMSCs and nbMSCs. Differentially expressed probesets were identified by a $\log_2$ fold change >1 and an adjusted p-value <0.05 (adjusted for multiple comparisons using false discovery rate). Differentially expressed genes were further analyzed for gene ontology term overrepresentation analysis using the BINGO plugin of Cytoscape [35] as well as functional annotation clustering using DAVID [36,37]. The data discussed in this publication have been deposited in NCBI's GeneExpression Omnibus [38] and are accessible through GEO Series accession number GSE142563 (https://www.ncbi.nlm.nih.gov/geo/query/acc.cgi?acc=GSE142563).

Western Blotting

Protein was isolated from MSCs cultured under standard conditions and then quantified by bicinchoninic acid (BCA) assay (Pierce, Rockford, IL, USA). Next, 25 µg of total protein was loaded onto SDS-polyacrylamide gel electrophoresis and transferred to nitrocellulose membranes. Membranes were blocked in 5% skimmed milk for 1 hour at room temperature and then incubated with primary antibody (antibodies against SLIT3, Abcam, ab78365, Cambridge, UK) overnight at 4 °C. Goat anti-rabbit IgG (H+L) 800 CW was applied for 1 hour at room temperature (1:5000, LI-COR Biosciences, Lincoln, NE). Visualization and quantification were carried out with the LI-COR Odyssey® scanner and software (LI-COR Biosciences).

Transgenic Mice.

Slit3$^{+/+}$ and *Slit3*$^{-/-}$ mice on a CD-1 background were obtained from Dr. Sean Mclean (University of North Carolina). *Robo1*$^{+/+}$ and *Robo1*$^{-/-}$ mice (CD-1 background) were obtained from Dr. Marc Tessier-Lavigne (Stanford University). Neonatal mice (n = 3-5 per genotype group) at postnatal day 8-10 were anesthetized with isoflurane, and the whole thymus was obtained for IHC studies for CD31, SLIT3, and ROBO1. Thymus tissue was fixed with 10% formalin and embedded in paraffin using standard protocols. The paraffin blocks were sectioned at 5 µm thickness. For immunohistochemistry, the sections were deparaffinized with xylene and rehydrated through a graded ethanol series of solutions. The sections were then subjected to heat-induced antigen retrieval in citrate buffer (pH 6.0), blocked with 5% BSA PBS buffer and incubated with primary antibodies at 4°C overnight. Anti-SLIT3 (1:100, Sigma-Aldrich, SAB2104337, St. Louis, MO), anti-ROBO1 (1:100, ab7279, Abcam, Cambridge, UK), and anti-CD31 (1:40, Novus Biologicals,

Littleton, CO, USA) antibodies were used. The appropriate secondary antibody Alexa Fluor® (ThermoFisher Scientific) were used at a dilution of 1:200. Hoechst was used for nuclear counterstaining and all sections were mounted in Prolong Diamond Antifade Mountant (ThermoFisher Scientific). Images were obtained by confocal microscopy (Nikon A1Si, Melville, NY, USA).

In a separate experiment, the thymus was removed from *Slit3*$^{+/+}$ and *Slit3*$^{-/-}$ neonatal mice (n = 8 per genotype group) and mechanically minced into 1- 2 mm pieces. Explant culture was then performed as described for the isolation of human ntMSCs [29]. After 7 to 10 days, tissue fragments were removed, and migrated MSCs from tissue fragments were cultured until they reached 80% confluence.

Statistical Analysis

Statistical analysis was performed using a ratio t test of paired data or unpaired two-tailed Student's t-test using GraphPad Prism 9 (GraphPad Software, La Jolla, CA) when appropriate, and $p<0.05$ was considered significant. Data are presented as mean ± SD.

RESULTS

Neonatal thymus and bone MSCs possess unique pericytic signatures

We previously determined that human ntMSCs and nbMSCs could undergo *in vitro* multilineage differentiation and shared many surface markers expressed by abMSCs [28,29]. To further characterize these neonatal MSCs, we determined the expression of surface markers that have

been previously associated with perivascular cells [39]. With flow cytometry, we observed that ntMSCs expressed higher levels of CD140b (PDGFRβ), lower levels of CD146 (MCAM/MUC18), equivalently low levels of CD140a (PDGFRα), and equivalently high levels of CD90 (Thy1) as compared to subject-matched nbMSCs (Fig. 1A and Supplementary Table S2). Furthermore, as compared to abMSCs and subject-matched nbMSCs, ntMSCs possessed a significantly higher transcript level of *TBX18* (Fig. 1B), which encodes for a transcription factor that is expressed in the perivascular cells of many organs in mice [8]. These results demonstrate that MSCs possess a tissue-specific pericytic phenotype.

Neonatal thymus MSCs are more proangiogenic than subject-matched nbMSCs.

After identifying that ntMSCs and nbMSCs possessed different pericytic signatures, we next assessed if ntMSCs would be functionally different than subject-matched nbMSCs in promoting neovascularization *in vitro* and *in vivo*. Since the primary mechanism by which MSCs stimulate angiogenesis is thought to be via the secretion of proangiogenic factors [40,41], we first determined if the secretome from these two types of MSCs would vary in their ability to promote HUVEC tube formation *in vitro*. HUVECs in Matrigel were exposed to conditioned medium obtained from ntMSC and nbMSC cultures. HUVEC tube and network formation were significantly increased in the group exposed to conditioned medium from ntMSCs as compared to that obtained from matched nbMSCs, as well as from cultures of unrelated abMSCs (Figs. 2A and 2B). We then observed that ntMSCs possessed increased transcript levels of the proangiogenic factors *VEGFA*, *FGF2*, *ANGPT1*, and *HIF1A* (Fig. 2C). The expression of *CXCL12* and *HGF*, both

of which have been shown to encode factors involved in bone marrow-derived MSC mediated angiogenesis [42,43], were similar to subject-matched nbMSCs (Fig. 2C). These results suggest that the secretome of ntMSCs is more proangiogenic than that of bone-derived MSCs.

Next, we determined the ability of ntMSCs and nbMSCs to promote angiogenesis in vivo by encapsulating them in a collagen-fibronectin plug along with HUVECs and then implanting them subcutaneously in NOD-SCID mice. Plugs were explanted after two weeks and were assessed for the presence of human CD31+ luminal structures containing red blood cells. We found that ntMSCs and HUVECs generated more perfused human CD31+ blood vessels as compared to nbMSCs and HUVECs (Figs. 2D and 2E). When compared to abMSCs, we also found that ntMSCs stimulated angiogenesis to a greater degree in vivo (Supplementary Figs. S1A and S1B). Collectively, these results indicate that MSCs isolated from the human neonatal thymus gland are more efficient in promoting angiogenesis *in vitro* and *in vivo* as compared to bone-derived MSCs.

Neonatal thymus MSCs are more motile and invasive than nbMSCs *in vitro*.

Perivascular cells such as MSCs are recruited and extend from adjacent areas to neovessels or capillaries that lack perivascular coverage [44,45], indicating that MSCs must be motile and be able to negotiate the extracellular matrix (ECM) to reach its appropriate destination. Further, MSCs must be motile and tissue invasive in order to home to areas of injury to impart their therapeutic effects [16].

Using a Boyden chamber assay, we first observed that ntMSCs had increased motility as compared to subject-matched nbMSCs (Fig. 3A). Next, we determined the ability of ntMSCs and

nbMSCs to invade and migrate through fibrin, a key component of the early provisional matrix that is important for tissue repair [46]. We used a spheroid invasion assay [29,47] and determined that ntMSCs invaded fibrin more rapidly than nbMSCs (Figs. 3B and 3C). Altogether, this pairwise comparison indicates that ntMSCs are consistently more motile and invasive than subject-matched nbMSCs.

Neonatal thymus MSCs have increased expression of SLIT3.

To further understand the mechanisms underlying the functional differences between ntMSCs and nbMSCs, we performed genome-wide profiling with microarray in pairs of MSCs isolated from 5 neonatal subjects. We found 116 genes that were at least 2x fold upregulated and 105 genes that were downregulated in ntMSCs as compared to nbMSCs (Fig. 4A, Supplementary Tables S3 and S4). Gene ontology category overrepresentation analysis revealed many processes related to tissue development in ntMSCs (Fig. 4B). Although functional annotation clustering did not identify any clusters related to angiogenesis, it did identify a cluster of genes (Annotation Cluster 5) enriched in ntMSCs that were related to axon guidance and Roundabout signaling (Supplementary Table S5), processes that have also been shown to regulate angiogenic sprouting [48,49]. Specifically, the secreted axon guidance molecule SLIT3 [50], also known to a proangiogenic factor [18,19], was found to be more highly expressed in ntMSCs (Supplementary Table S3), which we confirmed with qPCR and Western Blotting (Figs. 4C-E). Indeed, neutralizing SLIT3 in ntMSC conditioned medium with a specific antibody resulted in decreased HUVEC

network formation in vitro, indicating that SLIT3 contributes to the paracrine effects of ntMSCs (Fig. 4F and Fig. S2).

SLIT3 is important for neonatal thymus vascularity

Global deficiency of SLIT3 causes congenital diaphragmatic hernia in mice that is due to a defect diaphragmatic angiogenesis, however the impact of SLIT3 on the vascular beds of other tissues is unknown [18]. We first investigated the spatial expression of SLIT3 in murine neonatal thymus tissue since we had established that it was highly expressed in human ntMSCs. We found that SLIT3 is most dominantly in the peri-arteriolar region as well as within the stroma of the thymic cortex (Fig. 5A). Given the role of perivascular MSCs in thymus angiogenesis [51] and localization of SLIT3 expression to the perivascular cells in the neonatal thymus (Fig. 5A), we next postulated that SLIT3 played a role in thymus vascularization. To investigated this, we determined the CD31+ vascular density of thymus glands obtained from neonatal *Slit3*$^{+/+}$ and *Slit3*$^{-/-}$ mice. We found that vascular density was significantly decreased in thymus tissue from *Slit3* null mice (Figs. 5B and 5C). Altogether, these results confirm that SLIT3 is highly expressed in perivascular cells within the neonatal thymus gland and is important for thymus angiogenesis.

SLIT3 promotes the motile and invasive behavior of ntMSCs via ROBO1.

Given its ability to regulate the motility of various cell types [18,52-54], we investigated if SLIT3 could influence ntMSC invasive behavior in an autocrine fashion. We first determined the effects

of rhSLIT3 on ntMSC and nbMSC spheroids and found that it increased invasion in fibrin gel but as a collective migration from the central mass of the spheroid and not as individual sprouts (Fig. 6A). We next isolated ntMSCs from *Slit3*$^{-/-}$ mice and found that they demonstrated blunted invasive behavior as compared to ntMSCs from *Slit3*$^{+/+}$ mice (Fig. 6B). Given the possibility that SLIT3 deficiency may have interfered with the development (and subsequent ability to migrate and invade) of the ntMSCs from these global kockout mice, we targeted *SLIT3* transcription in human ntMSCs with siRNA and found that decreasing SLIT3 expression also resulted in decreased length and number of sprouts from ntMSC spheroids, indicating that SLIT3 can directly regulate postnatal MSC motility and invasion in an autocrine fashion (Fig. 6C).

Given that ROBO1 and ROBO4 are potential receptors for the SLIT3 ligand [18], we first evaluated the transcript expression of the genes for both of these receptors in human MSCs (Fig. 6D). We discovered that *ROBO1* transcript levels were up to 20-80 times more abundant than that of *ROBO4* transcripts in human MSCs (Fig. 6D). In the MSC pairs that we isolated from three patients, we found that ntMSCs had a higher ROBO1 transcript levels as compared to nbMSCs, but this was not significant (Fig. 6E). These results implied that ROBO1 (and not ROBO4) is likely the dominant receptor for SLIT3 in MSCs. To further confirm this, we targeted *ROBO1* transcription with specific siRNA and determined the effects on human ntMSC spheroid invasive sprouting. We found that targeting *ROBO1* transcription resulted in significantly decreased invasive ntMSC behavior (Fig. 6F). Altogether, these results demonstrate that SLIT3 promotes ntMSC invasion and motility in fibrin in an autocrine fashion via ROBO1.

ROBO1 participates in neonatal thymus angiogenesis.

The above findings indicated that MSCs can promote thymus angiogenesis via SLIT3 and that SLIT3 can act in an autocrine fashion to stimulate MSC motility and invasion. However, it is unclear how important MSC motility is to in vivo angiogenesis since sprouting is primarily formed by tip ECs [55]. To determine the presence of any relationship between ROBO1-mediated MSC motility and invasion and MSC-facilitated in vivo angiogenesis, we evaluated the vascularity of thymus glands from neonatal *Robo1*$^{+/+}$ and *Robo1*$^{-/-}$ mice. In wild-type mice, ROBO1 was found to be localized to the perivascular region of larger vessels, but not in the endothelium (Fig. 7A). ROBO1 deficiency resulted in a significantly decreased CD31+ blood vessel density within the cortex of the neonatal thymus gland (Fig. 7B and 7C), phenocopying the observations made in the thymus glands of *Slit3*$^{-/-}$ neonatal mice. Altogether, these results indicate that ROBO1 is important for neonatal thymus angiogenesis, in part by possibly mediating the autocrine effects of SLIT3 on ntMSC motility and invasion.

DISCUSSION

MSCs are currently being investigated in about 500 clinical trials for a variety of diseases [56]. The therapeutic activity of MSCs is thought to be in part due to its ability to secrete beneficial factors that promote survival, rejuvenation, and regeneration of diseased or stressed parenchymal cells [57]. A universal effect of exogenously transplanted MSCs is its ability to stimulate angiogenesis in the surrounding parenchyma, which may also contribute to the therapeutic effects of MSCs, especially in the setting of ischemia [58,59]. MSCs from a variety of tissues are being

investigated as therapeutic agents, and our findings indicate that tissue source may be an important factor in determining their potency.

Our results of subject-matched MSCs also reveal that the secreted axon guidance molecule SLIT3 contributes to the proangiogenic effects of ntMSCs and that increased expression of *SLIT3* may partly explain why these MSCs were consistently found to be more potent at promoting angiogenesis as compared to subject-matched nbMSCs. These findings are consistent with the results of a prior study based on a comparison of bone marrow-derived MSC lines from two different individuals, and the MSC line that had a higher expression of *SLIT3* was more proangiogenic [19]. SLIT3 is known to act in a paracrine fashion to stimulate ECs and sprouting angiogenesis [18]. Interestingly, our studies indicate that SLIT3 may also act in an autocrine fashion via ROBO1 to stimulate MSC invasion and motility. Therefore *SLIT3* expression in MSCs may be a surrogate of their therapeutic potency, as it can stimulate both angiogenesis and MSC homing. Furthermore, our transcriptome analysis suggests that the tissue-specific properties of ntSMCs may extend beyond a difference in proangiogenic qualities as ntMSCs may have tendencies towards tissue development, formation, and regeneration.

The thymus gland is a highly vascular organ that can regenerate after injury and stress, and a marked angiogenic response mediated by MSCs supports thymus regeneration [51,60]. Further, a distinguishing characteristic of the thymus is that the entire vasculature, from the artery to microvascular bed to vein, is completely invested by pericytes [31]. On the other hand, the vasculature and blood vascular sinusoids of the bone marrow have incomplete pericyte coverage, as with the vasculature from many other organs and tissues [30,32]. Our results suggest that ROBO1-mediated effects on MSCs, such as invasion and motility, are also important for thymus

vascularization, indicating that SLIT3 exerts an autocrine effect on MSCs (Figs. 6A and 6B) that is independent of its paracrine effects on ECs that is mediated via ROBO4 [18]. MSC and pericyte motility are needed for neoangiogenesis as these cells are recruited from adjacent blood vessels to stabilize neovessels in a PDGFβ–dependent fashion [61]. Therefore a defect in SLIT3-ROBO1 signaling may result in defective MSC recruitment to neovasculature, leading to decreased stability of neovasculature, ultimately leading to decreased vascular density, similar to what is seen in EC-specific PDGFβ deficient mice [61]. Although SLIT3 and ROBO1 expression are generally found in the perivascular region, future studies will need to directly investigate the contribution of the SLIT3-ROBO1 signaling activity in perivascular MSCs on thymus angiogenesis and development by specific targeting using conditional knockout mouse models.

Portions of the thymus gland are routinely removed during neonatal and infant cardiac surgery, and thus this tissue presents as an ample and untapped source of neonatal MSCs, which we have previously shown to have therapeutic effects [29,59,62,63]. The results of this study further support the ntMSC as an attractive candidate for cell therapy given their superior proangiogenic properties. Patients with congenital heart disease who undergo cardiac surgery in the neonatal or early infancy periods are at risk of developing medical conditions secondary to defective perfusion or angiogenesis, such as capillary rarefaction from ventricular pressure overload which can contribute to heart failure [64-66], cerebral damage from complications of cardiopulmonary bypass and cardiac surgery [67,68], and myocardial ischemia and eventual heart failure from coronary obstruction after surgery [69]. Conceivably, autologous MSCs can be isolated from discarded thymus tissue obtained during neonatal or infant cardiac surgery, expanded and cryopreserved *in vitro*, and then thawed and utilized when medically indicated.

In conclusion, our results have important implications for the translational efforts of MSCs into clinical therapy. MSC proangiogenic characteristics are tissue source-dependent and are related to the activity of an autocrine SLIT3-ROBO1 signaling axis. Neonatal thymus MSCs, which have high endogenous SLIT3-ROBO1 activity and proangiogenic behavior, warrants further evaluation as therapy for ischemic disease.

REFERENCES

1 Gupta PK, Chullikana A, Parakh R et al. A double blind randomized placebo controlled phase I/II study assessing the safety and efficacy of allogeneic bone marrow derived mesenchymal stem cell in critical limb ischemia [in English]. J Transl Med 2013;11.

2 Bura A, Planat-Benard V, Bourin P et al. Phase I trial: the use of autologous cultured adipose-derived stroma/stem cells to treat patients with non-revascularizable critical limb ischemia [in English]. Cytotherapy 2014;16(2):245-257.

3 Das AK, Bin Abdullah BJJ, Dhillon SS et al. Intra-arterial Allogeneic Mesenchymal Stem Cells for Critical Limb Ischemia are Safe and Efficacious: Report of a Phase I Study [in English]. World J Surg 2013;37(4):915-922.

4 Guhathakurta S, Subramanyan UR, Balasundari R et al. Stem cell experiments and initial clinical trial of cellular cardiomyoplasty. Asian Cardiovasc Thorac Ann 2009;17(6):581-586.

5 Heldman AW, DiFede DL, Fishman JE et al. Transendocardial mesenchymal stem cells and mononuclear bone marrow cells for ischemic cardiomyopathy: the TAC-HFT randomized trial. JAMA 2014;311(1):62-73.

6 Perin EC, Murphy MP, March KL et al. Evaluation of Cell Therapy on Exercise Performance and Limb Perfusion in Peripheral Artery Disease: The CCTRN PACE Trial (Patients With Intermittent Claudication Injected With ALDH Bright Cells). Circulation 2017;135(15):1417-1428.

7 Rigato M, Monami M, Fadini GP. Autologous Cell Therapy for Peripheral Arterial Disease: Systematic Review and Meta-Analysis of Randomized, Nonrandomized, and Noncontrolled Studies. Circ Res 2017;120(8):1326-1340.

8 Guimaraes-Camboa N, Cattaneo P, Sun Y et al. Pericytes of Multiple Organs Do Not Behave as Mesenchymal Stem Cells In Vivo. Cell Stem Cell 2017;20(3):345-359 e345.

9 Rafii S, Butler JM, Ding BS. Angiocrine functions of organ-specific endothelial cells. Nature 2016;529(7586):316-325.

10 Nolan DJ, Ginsberg M, Israely E et al. Molecular signatures of tissue-specific microvascular endothelial cell heterogeneity in organ maintenance and regeneration. Dev Cell 2013;26(2):204-219.

11 Chapel A, Bertho JM, Bensidhoum M et al. Mesenchymal stem cells home to injured tissues when co-infused with hematopoietic cells to treat a radiation-induced multi-organ failure syndrome. J Gene Med 2003;5(12):1028-1038.

12 Bronckaers A, Hilkens P, Martens W et al. Mesenchymal stem/stromal cells as a pharmacological and therapeutic approach to accelerate angiogenesis. Pharmacol Ther 2014;143(2):181-196.

13 Le Blanc K, Mougiakakos D. Multipotent mesenchymal stromal cells and the innate immune system. Nat Rev Immunol 2012;12(5):383-396.

14 Caplan AI. Why are MSCs therapeutic? New data: new insight. J Pathol 2009;217(2):318-324.

15 Karp JM, Teol GSL. Mesenchymal Stem Cell Homing: The Devil Is in the Details [in English]. Cell Stem Cell 2009;4(3):206-216.

16 Ullah M, Liu DD, Thakor AS. Mesenchymal Stromal Cell Homing: Mechanisms and Strategies for Improvement. iScience 2019;15:421-438.

17 Lu C, Li XY, Hu Y et al. MT1-MMP controls human mesenchymal stem cell trafficking and differentiation. Blood 2010;115(2):221-229.

18 Zhang B, Dietrich UM, Geng JG et al. Repulsive axon guidance molecule Slit3 is a novel angiogenic factor [in English]. Blood 2009;114(19):4300-4309.

19 Paul JD, Coulombe KLK, Toth PT et al. SLIT3-ROBO4 activation promotes vascular network formation in human engineered tissue and angiogenesis in vivo [in English]. J Mol Cell Cardiol 2013;64:124-131.

20 Crisan M, Corselli M, Chen WC et al. Perivascular cells for regenerative medicine. J Cell Mol Med 2012;16(12):2851-2860.

21 Efimenko A, Dzhoyashvili N, Kalinina N et al. Adipose-Derived Mesenchymal Stromal Cells From Aged Patients With Coronary Artery Disease Keep Mesenchymal Stromal Cell Properties but Exhibit Characteristics of Aging and Have Impaired Angiogenic Potential [in English]. Stem Cell Transl Med 2014;3(1):32-41.

22 Efimenko AY, Kochegura TN, Akopyan ZA et al. Autologous Stem Cell Therapy: How Aging and Chronic Diseases Affect Stem and Progenitor Cells [in English]. Bioresearch Open Acc 2015;4(1):26-38.

23 Choudhery MS, Khan M, Mahmood R et al. Bone marrow derived mesenchymal stem cells from aged mice have reduced wound healing, angiogenesis, proliferation and anti-apoptosis capabilities [in English]. Cell Biology International 2012;36(8):747-753.

24 Khan M, Mohsin S, Khan SN et al. Repair of senescent myocardium by mesenchymal stem cells is dependent on the age of donor mice [in English]. J Cell Mol Med 2011;15(7):1515-1527.

25 Rasmussen JG, Frobert O, Holst-Hansen C et al. Comparison of human adipose-derived stem cells and bone marrow-derived stem cells in a myocardial infarction model. Cell Transplant 2014;23(2):195-206.

26 Fijany A, Sayadi LR, Khoshab N et al. Mesenchymal stem cell dysfunction in diabetes. Mol Biol Rep 2019;46(1):1459-1475.

27 Paladino FV, Peixoto-Cruz JS, Santacruz-Perez C et al. Comparison between isolation protocols highlights intrinsic variability of human umbilical cord mesenchymal cells. Cell Tissue Bank 2016;17(1):123-136.

28 Wang S, Mundada L, Colomb E et al. Mesenchymal Stem/Stromal Cells from Discarded Neonatal Sternal Tissue: In Vitro Characterization and Angiogenic Properties. Stem Cells Int 2016;2016:5098747.

29 Wang S, Mundada L, Johnson S et al. Characterization and angiogenic potential of human neonatal and infant thymus mesenchymal stromal cells. Stem Cells Transl Med 2015;4(4):339-350.

30 Armulik A, Abramsson A, Betsholtz C. Endothelial/pericyte interactions. Circ Res 2005;97(6):512-523.

31 Muller SM, Stolt CC, Terszowski G et al. Neural crest origin of perivascular mesenchyme in the adult thymus. J Immunol 2008;180(8):5344-5351.

32 Zetterberg E, Vannucchi AM, Migliaccio AR et al. Pericyte coverage of abnormal blood vessels in myelofibrotic bone marrows. Haematologica 2007;92(5):597-604.

33 Foster K, Sheridan J, Veiga-Fernandes H et al. Contribution of neural crest-derived cells in the embryonic and adult thymus. J Immunol 2008;180(5):3183-3189.

34 Sheng G. The developmental basis of mesenchymal stem/stromal cells (MSCs). BMC Dev Biol 2015;15:44.

35 Maere S, Heymans K, Kuiper M. BiNGO: a Cytoscape plugin to assess overrepresentation of gene ontology categories in biological networks. Bioinformatics 2005;21(16):3448-3449.

36 Huang da W, Sherman BT, Lempicki RA. Systematic and integrative analysis of large gene lists using DAVID bioinformatics resources. Nat Protoc 2009;4(1):44-57.

37 Huang da W, Sherman BT, Lempicki RA. Bioinformatics enrichment tools: paths toward the comprehensive functional analysis of large gene lists. Nucleic Acids Res 2009;37(1):1-13.

38 Edgar R, Domrachev M, Lash AE. Gene Expression Omnibus: NCBI gene expression and hybridization array data repository. Nucleic Acids Res 2002;30(1):207-210.

39 Ferland-McCollough D, Slater S, Richard J et al. Pericytes, an overlooked player in vascular pathobiology. Pharmacol Ther 2017;171:30-42.

40 Kwon HM, Hur SM, Park KY et al. Multiple paracrine factors secreted by mesenchymal stem cells contribute to angiogenesis. Vascul Pharmacol 2014;63(1):19-28.

41 Kuchroo P, Dave V, Vijayan A et al. Paracrine factors secreted by umbilical cord-derived mesenchymal stem cells induce angiogenesis in vitro by a VEGF-independent pathway. Stem Cells Dev 2015;24(4):437-450.

42 Zhang L, Zhou Y, Sun X et al. CXCL12 overexpression promotes the angiogenesis potential of periodontal ligament stem cells. Sci Rep 2017;7(1):10286.

43 Crisostomo PR, Wang Y, Markel TA et al. Human mesenchymal stem cells stimulated by TNF-alpha, LPS, or hypoxia produce growth factors by an NF kappa B- but not JNK-dependent mechanism. Am J Physiol Cell Physiol 2008;294(3):C675-682.

44 Jain RK. Molecular regulation of vessel maturation. Nat Med 2003;9(6):685-693.

45 Berthiaume AA, Grant RI, McDowell KP et al. Dynamic Remodeling of Pericytes In Vivo Maintains Capillary Coverage in the Adult Mouse Brain. Cell Rep 2018;22(1):8-16.

46 Barker TH, Engler AJ. The provisional matrix: setting the stage for tissue repair outcomes. Matrix Biol 2017;60-61:1-4.

47 De Wever O, Hendrix A, De Boeck A et al. Single cell and spheroid collagen type I invasion assay. Methods Mol Biol 2014;1070:13-35.

48 Adams RH, Eichmann A. Axon guidance molecules in vascular patterning. Cold Spring Harb Perspect Biol 2010;2(5):a001875.

49 Larrivee B, Freitas C, Suchting S et al. Guidance of vascular development: lessons from the nervous system. Circ Res 2009;104(4):428-441.

50 Brose K, Bland KS, Wang KH et al. Slit proteins bind Robo receptors and have an evolutionarily conserved role in repulsive axon guidance. Cell 1999;96(6):795-806.

51 Lax S, Ross EA, White A et al. CD248 expression on mesenchymal stromal cells is required for post-natal and infection-dependent thymus remodelling and regeneration. FEBS Open Bio 2012;2:187-190.

52 Tanno T, Fujiwara A, Sakaguchi K et al. Slit3 regulates cell motility through Rac/Cdc42 activation in lipopolysaccharide-stimulated macrophages. FEBS Lett 2007;581(5):1022-1026.

53 Zhang C, Guo H, Li B et al. Effects of Slit3 silencing on the invasive ability of lung carcinoma A549 cells. Oncol Rep 2015;34(2):952-960.

54 Schubert T, Denk AE, Ruedel A et al. Fragments of SLIT3 inhibit cellular migration. Int J Mol Med 2012;30(5):1133-1137.

55 Gerhardt H, Golding M, Fruttiger M et al. VEGF guides angiogenic sprouting utilizing endothelial tip cell filopodia. J Cell Biol 2003;161(6):1163-1177.

56 Squillaro T, Peluso G, Galderisi U. Clinical Trials With Mesenchymal Stem Cells: An Update. Cell Transplant 2016;25(5):829-848.

57 Fu Y, Karbaat L, Wu L et al. Trophic Effects of Mesenchymal Stem Cells in Tissue Regeneration. Tissue Eng Part B Rev 2017;23(6):515-528.

58 Tao HY, Han ZB, Han ZC et al. Proangiogenic Features of Mesenchymal Stem Cells and Their Therapeutic Applications [in English]. Stem Cells International 2016.

59 Wang S, Huang S, Gong L et al. Human Neonatal Thymus Mesenchymal Stem Cells Promote Neovascularization and Cardiac Regeneration. Stem Cells Int 2018;2018:8503468.

60 Park HJ, Kim MN, Kim JG et al. Up-regulation of VEGF expression by NGF that enhances reparative angiogenesis during thymic regeneration in adult rat [in English]. Bba-Mol Cell Res 2007;1773(9):1462-1472.

61 Lindblom P, Gerhardt H, Liebner S et al. Endothelial PDGF-B retention is required for proper investment of pericytes in the microvessel wall. Genes Dev 2003;17(15):1835-1840.

62 Sondergaard CS, Hodonsky CJ, Khait L et al. Human thymus mesenchymal stromal cells augment force production in self-organized cardiac tissue. Ann Thorac Surg 2010;90(3):796-803; discussion 803-794.

63 Chery J, Huang S, Gong L et al. Human Neonatal Thymus Mesenchymal Stem/Stromal Cells and Chronic Right Ventricle Pressure Overload. Bioengineering (Basel) 2019;6(1).

64 Friehs I, Moran AM, Stamm C et al. Promoting angiogenesis protects severely hypertrophied hearts from ischemic injury. Ann Thorac Surg 2004;77(6):2004-2010; discussion 2011.

65 Kitahori K, He H, Kawata M et al. Development of left ventricular diastolic dysfunction with preservation of ejection fraction during progression of infant right ventricular hypertrophy. Circ Heart Fail 2009;2(6):599-607.

66 Wehman B, Kaushal S. The emergence of stem cell therapy for patients with congenital heart disease. Circ Res 2015;116(4):566-569.

67 Maeda T, Sarkislali K, Leonetti C et al. Impact of Mesenchymal Stromal Cell Delivery Through Cardiopulmonary Bypass on Postnatal Neurogenesis. Ann Thorac Surg 2019.

68 Beca J, Gunn JK, Coleman L et al. New white matter brain injury after infant heart surgery is associated with diagnostic group and the use of circulatory arrest. Circulation 2013;127(9):971-979.

69 Goldsmith MP, Allan CK, Callahan R et al. Acute coronary artery obstruction following surgical repair of congenital heart disease. J Thorac Cardiovasc Surg 2019.

FIGURE TITLES AND LEGENDS

Figure 1. Pericytic signature of human neonate-matched MSCs.

A, Neonatal thymus MSCs possessed a surface marker expression as determined by flow cytometry that was more pericyte-like as compared to nbMSCs (also see Table S1, n=3 subjects). B, Transcript expression of perivascular cell-associated factor *TBX18* in subject-matched ntMSCs and nbMSCs as determined by qPCR. Each data pair represents ntMSCs and nbMSCs that were isolated from a single patient and all data compared with a ratio t test.

Figure 2. **Neonatal thymus MSCs are more proangiogenic than subject-matched nbMSCs.**

A, Conditioned medium (CM) from ntMSCs promoted greater HUVEC network formation as conditioned medium from nbMSCs and abMSCs. Scale bar = 200 μm. B, Quantification of HUVEC network formation in A. Each data point represents a randomly selected field of analysis. (Results are from n=3 subjects). C, Neonatal thymus MSCs had greater transcript levels of *ANGPT1* and *HIF1A* as compared to matched nbMSCs. Each data pair represents ntMSCs and nbMSCs that were isolated from a single patient and all data compared with a ratio t test. D, CD31 immunohistochemistry of MSC/HUVEC-seeded collagen/fibronectin constructs implanted in NOD SCID mice for 14 days. Scale bars = 50 μm. E, Quantification of CD31 vascular density of constructs in D, showing that ntMSCs stimulated more angiogenesis in vivo (n=5 animals with two constructs per animal; ntMSCs and nbMSCs isolated from the same subject). Each data point represents a randomly selected field of analysis.

Figure 3. Neonatal thymus MSCs are more invasive and motile than bone MSCs.

A, Quantification of Boyden chamber assay results for subject-matched ntMSCs and nbMSCs (n=3 subjects). Each data point represents the average of four technical replicates for each cell line and averaged data points were compared with a ratio t test. B, Spheroid comprised of ntMSCs manifested more sprouting/invasion in fibrin as compared to those made with matched nbMSCs. Scale bars = 100 μm. C, Quantification of number and length of branches from spheroids in B (n=3 subjects) with each data point representing analysis from a single, independent spheroid.

Figure 4. SLIT3 is upregulated in ntMSCs and is important for their proangiogenic paracrine effects. A, Heatmap of differentially expressed genes in subject-matched ntMSCs and nbMSCs as determined by microarray (also see Supplementary Tables S3 and S4, n=5 subjects). B, Network of gene ontology overrepresentation analysis of overexpressed genes in ntMSCs (Supplementary Table S3) indicate enrichment for development and morphogenesis processes. C, *SLIT3* transcript expression in subject-matched ntMSCs and nbMSCs as determined by qPCR. Each data pair represents ntMSCs and nbMSCs that were isolated from a single patient. D and E, SLIT3 expression in subject-matched ntMSCs and nbMSCs as determined by Western blotting with quantification (results are representative of n=2 subjects). F, Neutralizing SLIT3 in the conditioned medium (CM) obtained from ntMSCs decreases their ability to promote HUVEC network formation in vitro. Experiments were performed wtih conditioned medium generated from three different ntMSC lines. Three random fields were analyzed per group, averaged, and then compared with a Student's t test.

Figure 5. SLIT3 is important for neonatal thymus angiogenesis. A, Immunohistochemistry of wildtype *Slit3*$^{+/+}$ mouse neonatal thymus gland showing localization of SLIT3 to the perivascular region of arterioles (results representative of samples from n=3 animals). Scale bars = 50 μm. B

and C, CD31 immunohistochemistry of thymus glands from *Slit3*$^{+/+}$ and *Slit3*$^{-/-}$ neonatal mice with quantification of CD31 vascular density (n=5 thymus glands per group). Each data point represents a randomly selected field of analysis. Scale bars= 60 μm.

Figure 6. ROBO1 mediates SLIT3 invasive motile effects on ntMSCs. A, Recombinant human SLIT3 promotes a general spreading of ntMSC spheroids in fibrin gel. B, ntMSCs from *Slit3*$^{-/-}$ neonatal mice have decreased invasive motile activity than ntMSCs from *Slit3*$^{+/+}$ neonatal mice. ntMSCs were pooled from n=8 animals/genotype group. C, Targeting *SLIT3* transcription with siRNA inhibits ntMSC spheroid invasive sprouting. D, *ROBO1* is expressed 20-80 times more than *ROBO4* in MSCs. Each data pair represents ntMSCs and nbMSCs that were isolated from a single patient and data were compared with a ratio t test. E, *ROBO1* transcript levels in paired human nbMSCs and ntMSCs as determined by qPCR and data were compared with a ratio t test. Each data pair represents ntMSCs and nbMSCs that were isolated from a single patient. F, Targeting *ROBO1* transcription with siRNA inhibits ntMSC spheroid invasive sprouting. Spheroid experiment results (A, C, and F) are representative of at least four independent experiments utilizing MSCs isolated from n=4 subjects. Data points for qPCR of siRNA treated MSCs represent technical replicates and data points for spheroid branching analysis represent a single spheroid. Spheroid experimental results were analyzed with a Student's t test. Scale bars = 100 μm.

Figure 7. ROBO1 participates in neonatal thymus angiogenesis. A, Immunohistochemistry of wildtype *Robo1*$^{+/+}$ mouse neonatal thymus gland showing localization of ROBO1 to the perivascular region of arterioles (Results representative tissue from n=3 animals). Scale bars = 10 μm. B and C, CD31 immunohistochemistry of thymus glands from *Robo1*$^{+/+}$ and *Robo1*$^{-/-}$ neonatal mice with quantification of CD31 vascular density (At least n=5 sections were analyzed

from n=3 thymus glands per genotype group). Each data point represents a randomly selected field of analysis. Scale bars = 60 μm.

SUPPLEMENTARY FIGURES AND TABLES

Supplementary Figure S1. Neontatal thymus MSCs was superior to adult bone marrow-derived MSCs in promoting angiogenesis in vivo. A and B, CD31 immunohistochemistry of abMSC/HUVEC-seeded collagen/fibronectin (A) and ntMSC/HUVEC-seeded collagen/fibronectin (B) constructs implanted in NOD SCID mice for 14 days. Scale bars = 50 μm. Only 20% (1/5 constructs) of explanted constructs from the abMSC/HUVEC group demonstrated CD31 positive luminal structures whereas 100% of ntMSC/HUVEC constructs possessed numerous CD31 positive vessels (n=5 animals with two constructs per animal).

Supplementary Figure S2. Neutralizing SLIT3 in the conditioned medium (CM) obtained from ntMSCs decreases their ability to promote HUVEC network formation in vitro. A specific anti-SLIT3 antibody can decrease the ability of conditioned medium from ntMSCs to promote HUVEC network formation in vitro. Data from these experiments are quantified and analyzed in Fig. 4F.

Supplementary Table S1. qPCR primers used in this study.

Supplementary Table S2. Pericytic surface marker expression of three subject-matched neonatal thymus and bone MSCs as determined by flow cytometry.

Supplementary Table S3. Upregulated genes (> 2.0x fold) in ntMSCs as compared to subject-matched nbMSCs as determined by microarray analysis.

Supplementary Table S4. Down-regulated genes in ntMSCs as compared to subject-matched nbMSCs determined by microarray analysis.

Supplementary Table S5. Functional annotation analysis using DAVID of overexpressed genes in ntMSCs as identified by microarray.

Supplementary Table S6. Details of the cell lines and subjects.

Supplementary Table S7. Specific cell lines used in each experiment.

Supplementary Table S8. Individual data values and cell lines used for qPCR gene expression shown in Figs. 1B, 2C, 4C, 6D, and 6E.

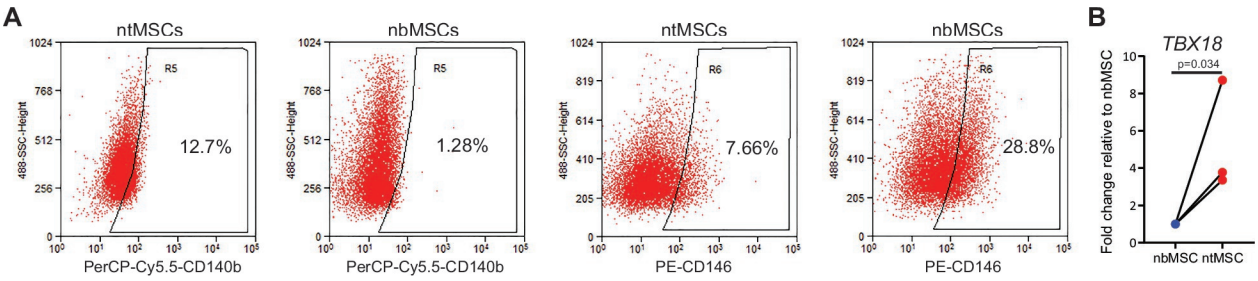

sct3_12723_figure 1 msc comparison paper r1.eps

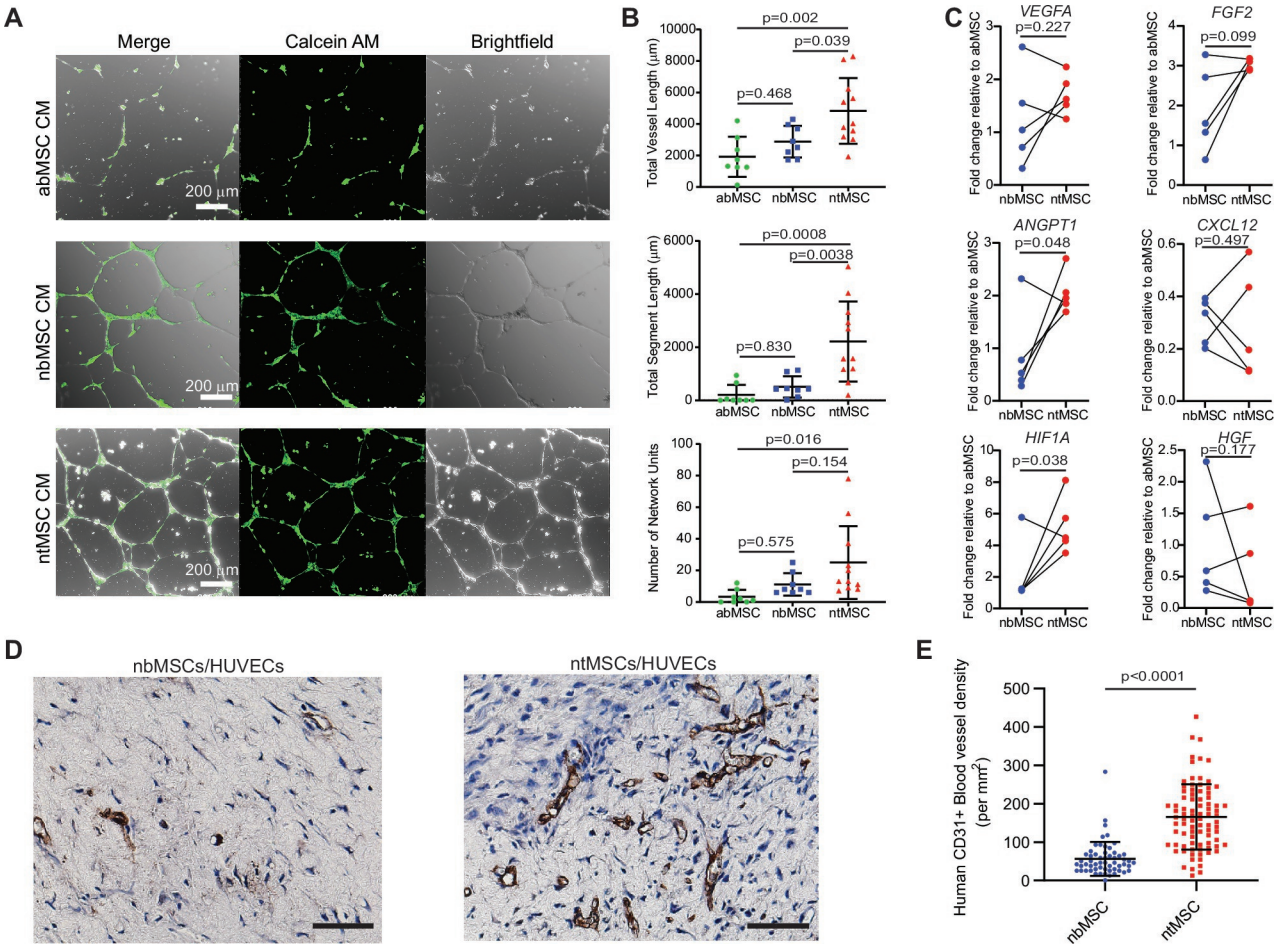

sct3_12723_figure 2 msc comparison paper r1_05.03.20.eps

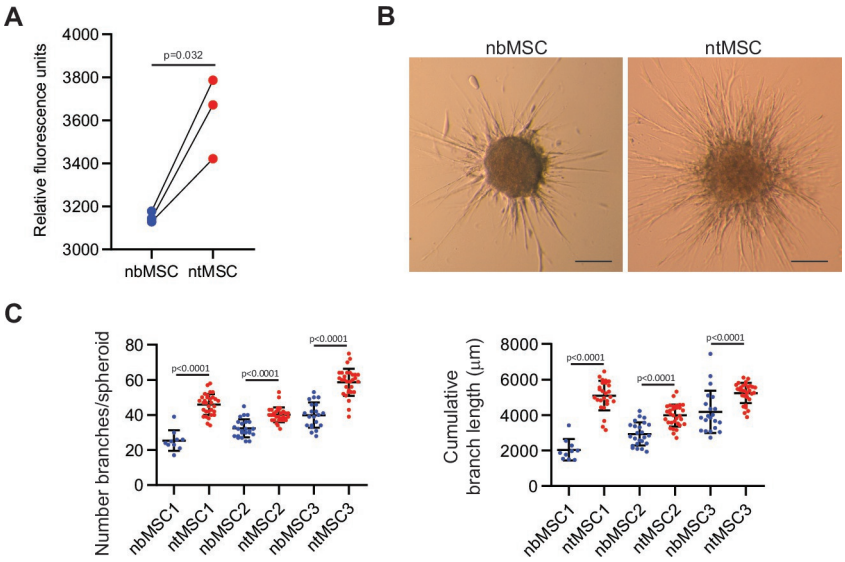

sct3_12723_figure 3 msc comparison paper r1.eps

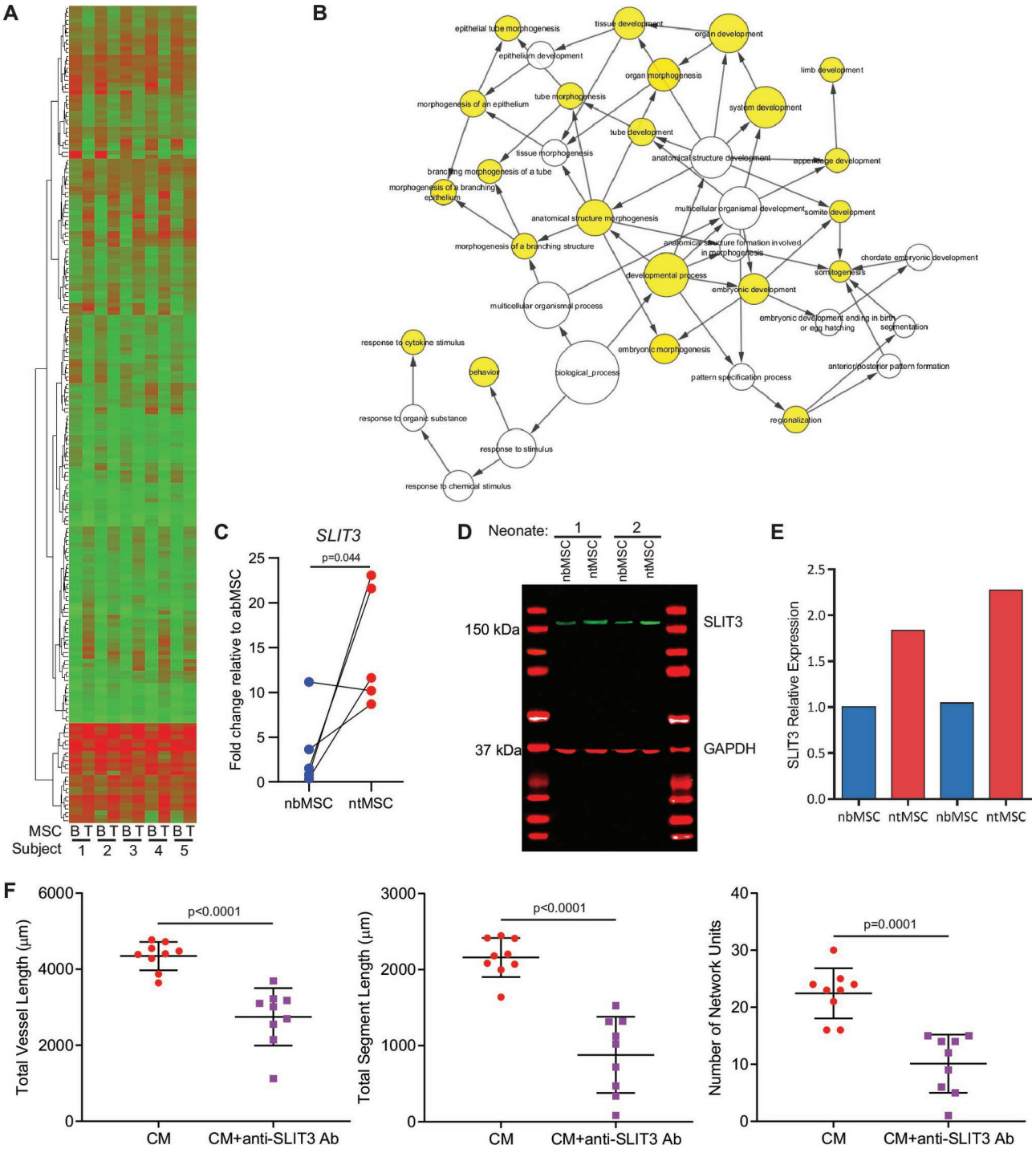

sct3_12723_figure 4 msc slit3 r1_5.3.20.eps

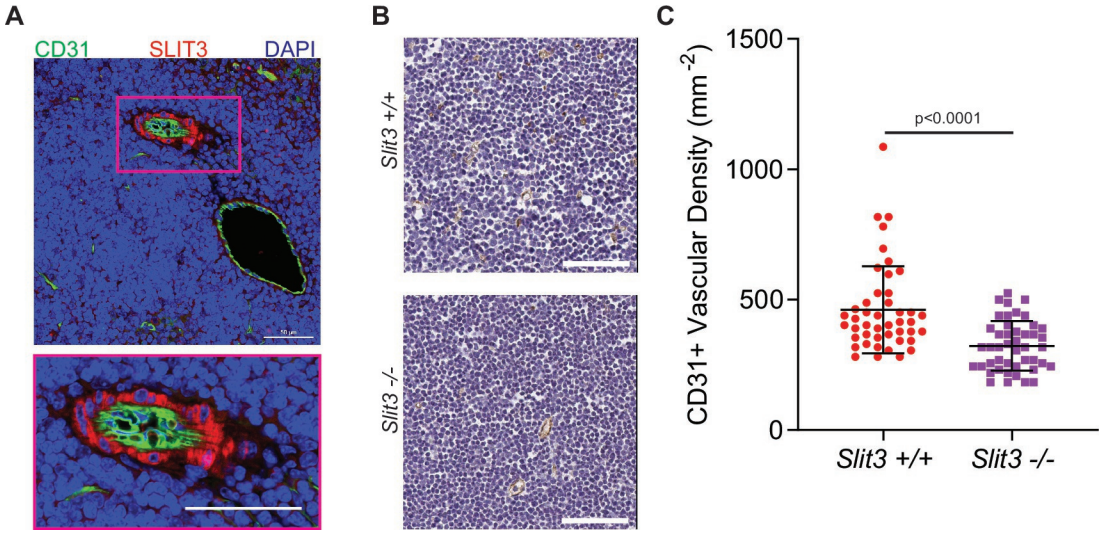

sct3_12723_figure 5 msc comparison paper_r1.eps

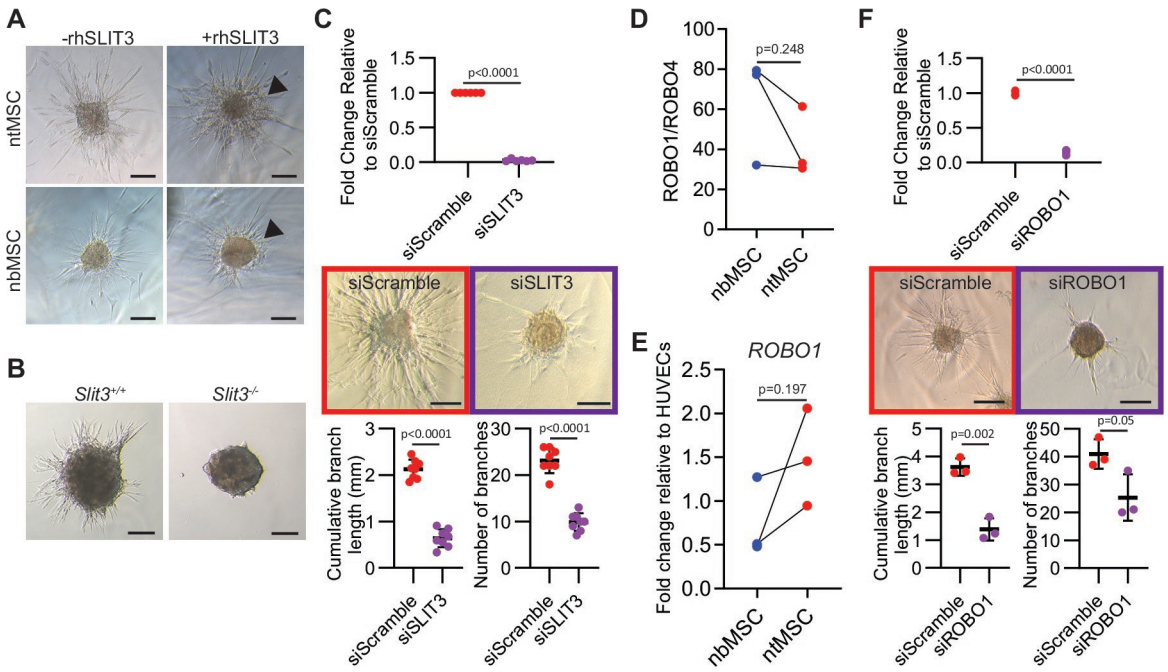

sct3_12723_figure 6 msc comparison paper r1.eps

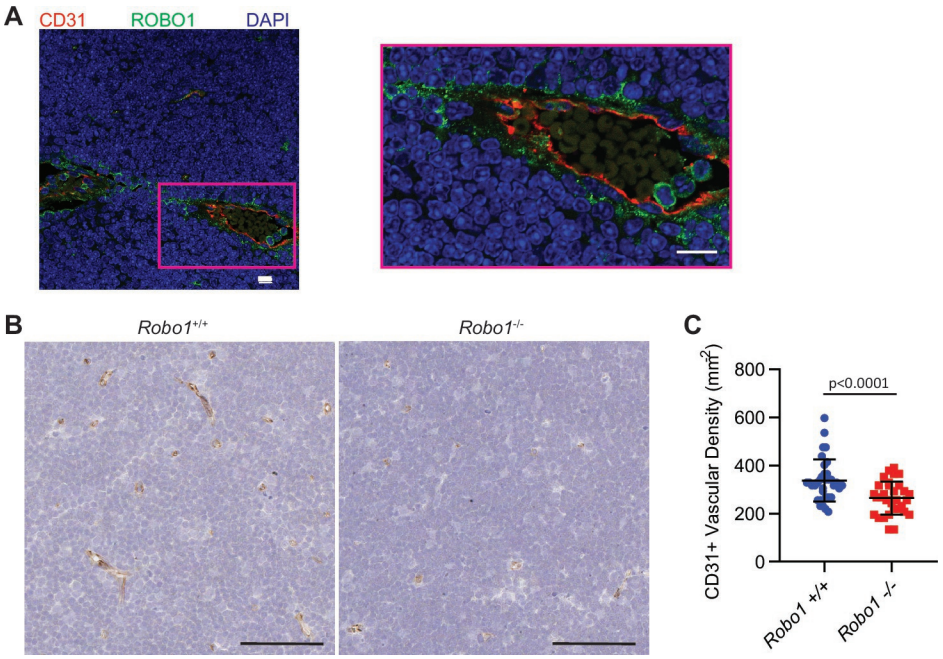

sct3_12723_figure 7 msc comparison paper_5.3.20.eps

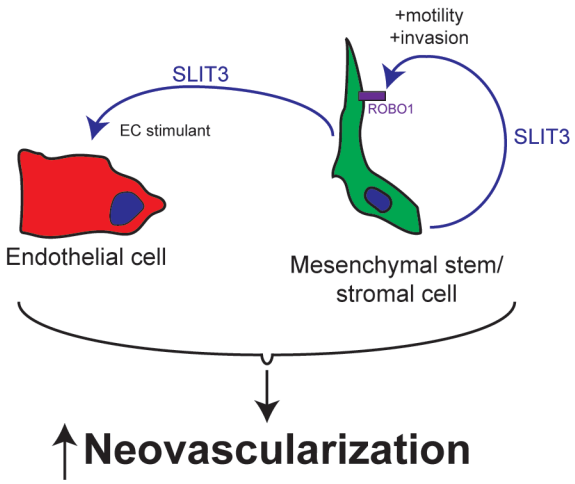

SCT3_12723_Graphical Abstract MSC comparison paper_12.11.19.tif

TITLE: Tissue-Specific Angiogenic and Invasive Properties of Human Neonatal Thymus and Bone MSCs: Role of SLIT3-ROBO1

RUNNING HEAD: Role of SLIT3-ROBO1 in MSCs

AUTHORS: Shuyun Wang,[1] Shan Huang,[1] Sean Johnson,[1] Vadim Rosin,[1] Jeffrey Lee,[1] Eric Colomb,[1] Russell Witt,[2] Alexander Jaworski,[3] Stephen J. Weiss,[4] Ming-Sing Si,[1]

AFFILIATIONS: [1]Department of Cardiac Surgery, Section of Pediatric Cardiovascular Surgery, University of Michigan, Ann Arbor, MI 48109, USA; [2]Department of General Surgery, Brigham and Women's Hospital, MA 02115, USA; [3]Department of Neuroscience, Brown University, Providence, RI 02912, USA; [4]Department of Internal Medicine, University of Michigan, Ann Arbor, MI 48109, USA.

AUTHOR CONTRIBUTIONS:
Shuyun Wang: Collection and assembly of data, data analysis and interpretation, and manuscript writing.
Shan Huang: Collection and assembly of data.
Sean Johnson: Collection and assembly of data.
Vadim Rosin: Collection and assembly of data and data analysis and interpretation.
Jeffrey Lee: Collection and assembly of data.
Eric Colomb: Collection and assembly of data.
Russell Witt: Collection and assembly of data.
Alexander Jaworski: Provision of study material and manuscript writing.
Stephen J. Weiss: Conceptin and design, data analysis and interpretation, manuscript writing, and final approval of manuscript.
Ming-Sing Si: Conception and design, financial support, provision of study materials, collection and assembly of data, data analysis and interpretation, manuscript writing, and final approval of manuscript.

CORRESPONDENCE INFORMATION:
Ming-Sing Si, MD
University of Michigan
C.S. Mott Children's Hospital
Department of Cardiac Surgery
Floor 11, Room 735
1540 E. Hospital Drive
Ann Arbor, Michigan 48109
mingsing@umich.edu

ACKNOWLEDGEMENTS: Research reported in this publication was partially supported by the National Heart, Lung, And Blood Institute of the National Institutes of Health under Award Number K08HL146351 The content is solely the responsibility of the authors and does not necessarily represent the official views of the National Institutes of Health. Other support for this work was from the University of Michigan Department of Cardiac Surgery, University of

Michigan Frankel Cardiovascular Center, Faith's Angels, and the Children's Heart Foundation. Assistance from the University of Michigan DNA Microarray Core is acknowledged.

CONFLICTS OF INTEREST: Authors have none to disclose.

KEY WORDS: Mesenchymal stem cells, SLIT3, ROBO1, cell motility, angiogenesis

ABSTRACT

While MSCs are being explored in numerous clinical trials as proangiogenic and proregenerative agents, the influence of tissue origin on the therapeutic qualities of these cells is poorly understood. Complicating the functional comparison of different types of MSCs are the confounding effects of donor age, genetic background, and health status of the donor. Leveraging a clinical setting where MSCs can be simultaneously isolated from discarded but healthy bone and thymus tissues from the same neonatal patients, thereby controlling for these confounding factors, we performed an *in vitro* and *in vivo* paired comparison of these cells. We found that both neonatal thymus (nt)MSCs and neonatal bone (nb)MSCs expressed different pericytic surface marker profiles. Further, ntMSCs were more potent in promoting angiogenesis *in vitro* and *in vivo* and they were also more motile and efficient at invading ECM *in vitro*. These functional differences were in part mediated by an increased ntMSC expression of SLIT3, a factor known to activate endothelial cells. Further, we discovered that SLIT3 stimulated MSC motility and fibrin gel invasion via ROBO1 in an autocrine fashion. Consistent with our findings in human MSCs, we found that SLIT3 and ROBO1 were expressed in the perivascular cells of the neonatal murine thymus gland and that global SLIT3 or ROBO1 deficiency resulted in decreased neonatal murine thymus gland vascular density. In conclusion, ntMSCs possess increased proangiogenic and invasive behaviors which are in part mediated by the paracrine and autocrine effects of SLIT3.

INTRODUCTION

Mesenchymal stem/stromal cells (MSCs) are located in the perivascular region, can be isolated from a variety of tissues, and are being evaluated as proangiogenic and proregenerative therapies in numerous clinical trials [1-8]. While endothelial cells have been recently recognized to possess tissue-specific properties, the influence of tissue origin on MSC therapeutic effects is poorly understood [9,10].

The ability of MSCs to migrate to damaged tissues to exert its proregenerative, antiinflammatory and proangiogenic effects also influences their therapeutic potential [11-14]. Infusion of MSCs into the venous circulation result in intravascular homing to injured areas, and homing over shorter distances through the tissue interstitium are also likely to occur in the setting of local injection [15,16]. Requisite for homing is the motile and tissue-invasive abilities of MSCs, and the influence of tissue origin on these characteristics is not known [17]. The secreted axon guidance molecule SLIT3 has been shown to be an endothelial cell (EC) stimulant [18] and has been associated with a bone marrow derived MSC line that is proangiogenic [19]; however, it is not known if this finding can be generalized to other MSC lines.

Knowing these tissue-specific properties of MSCs is important because they may have translational implications for MSC therapies [20]. However, comparing MSCs from different tissues is confounded by factors such as donor age, presence of systemic disease, and individual variability [21-27]. We have been able to simultaneously isolate MSCs from thymus and bone tissue from neonates undergoing cardiac surgery, thereby allowing for a paired comparison that controls for the above confounding factors [28,29]. These two tissues have disparate perivascular mural cell embryological origin and different degrees of perivascular mural cell coverage of the vasculature [30-34]. Based on these differences, we hypothesized that MSCs from the thymus and bone would have different proangiogenic, motile, and invasive characteristics. Using both *in*

vitro and *in vivo* assays, we evaluated this hypothesis and identified that SLIT3 contributes to the observed differences in these functional properties of MSCs.

MATERIALS AND METHODS

Cell Isolation and Culture

Isolation, culture, and characterization of the human ntMSCs and nbMSCs used in these studies were previously described [28,29] under a protocol that was approved by the University of Michigan Institutional Review Board. Furthermore, Human adult bone marrow-derived (ab)MSCs were obtained from Lonza (Basel, Switzerland) and ATCC (Manassas, VA, USA), and human umbilical vein endothelial cells (HUVECs) were obtained from Lonza. Unless specified otherwise, all experiments utilized cells from passages 3-9.

Pericytic Signature Analysis

Pericyte surface markers of ntMSCs and nbMSCs isolated from n=3 patients were characterized by flow cytometry using fluorochrome-conjugated anti-human CD140a, CD140b, CD146, and CD90 (BD Biosciences, San Jose, CA). The antibodies were incubated with MSCs for 60 minutes at room temperature followed by three washes. MSCs were then analyzed using a MoFlo® Astrios™ flow cytometer (Beckman Coulter, Inc., Pasadena, CA, USA) using the appropriate isotype-matched and unstained controls.

We also measured the transcript expression of *TBX18*, recently determined to be expressed in the perivascular mural cells of mice vasculature [8], in human ntMSCs, nbMSCs, and abMSCs using qPCR (see below).

MSC Conditioned Medium Generation and HUVEC Tube Formation Assay

Ninety-six-well plates were coated with 60 µl Matrigel matrix (10 mg/mL, Corning, NY, USA) per well at 37°C for 30 to 60 minutes. HUVEC suspensions were prepared using the corresponding medium at a concentration of 1.5 x 10^5 /mL. Next, 100 µl (15,000) of cells were added to each well (5 wells per group) on top of the gelled Matrigel followed by the addition of 100 µl of MSC conditioned medium and then incubated at 37°C, 5% CO_2 for 4 to 16 hours. Once tube formation was observed, the plate was washed with HBSS, and the cells were labeled with Calcein AM (2 µM) (ThermoFisher Scientific, Waltham, MA, USA) for 30 min at 37°C in 5% CO_2 and were photographed using a fluorescent microscope. In subsequent experiments, a blocking anti-SLIT3 antibody (5 µg/mL, AF3629, R&D Systems, Minneapolis, MN, USA) was added to the ntMSC derived conditioned medium to neutralize the effects of SLIT3.

Boyden Chamber Assay

Mesenchymal stromal cell migration was measured using the Boyden chamber assay (Cell Biolabs, Inc., San Diego, CA, USA) in a 24-well format with 8 µm pore size according to the manufacturer's instructions. In brief, 5 x 10^4 cells in 300 µl serum-free medium were seeded in the upper compartment (the insert) and then allowed to migrate through the pores of the membrane into the lower compartment. After an appropriate incubation time in a cell culture incubator, migratory cells on the bottom of the polycarbonate membrane were stained and quantified in a fluorescence plate reader.

***In Vitro* Spheroid Angiogenic Sprouting Assay**

Spheroids comprised of 800 MSCs or 400 MSCs/400ECs were generated by hanging drop culture as previously described [29]. Spheroids were embedded in fibrin gel and allowed to sprout for 20 hours. Brightfield images were then acquired digitally and were analyzed using NeuronJ as previously described [29]. In some experiments, rhSLIT3 (12.5 µg/ml) (R&D Systems, Minneapolis, MN, USA) was added to the media just after spheroids were embedded in fibrin gel.

In other experiments, *SLIT3* or *ROBO1* gene targeting in MSCs was performed using siRNA (Origene, Rockville, MD, USA). Knockdown of gene expression was confirmed by qPCR before use in experiments, and experiments were repeated with at least two different siRNAs.

qPCR

Differential gene was performed using qPCR. RNA from cells was extracted according to the manufacturer's instructions using the RNeasy Mini Kit (Qiagen, Hilden, Germany) and 1 µg of total RNA was reverse transcribed with qScript cDNA Synthesis Kit (Quantabio, Beverly, MA, USA). Quantitative polymerase chain reactions were carried out with PerfeCTa SYBR Green supermix (Quantabio) and the Applied Biosystems (Foster City, CA USA), QuantStudio 5 Real-Time PCR System. Data were analyzed using the $2^{-\Delta\Delta C_T}$ method. The genes and primers used for this study are listed in Supplementary Table S1.

***In Vivo* Angiogenesis Assay**

The care of animals was in accordance with institutional guidelines. Constructs (n=5/group) containing 2 million cells (HUVECs, MSCs, and HUVECs/MSCs at a 1:1 ratio) or no cells (control group) were made in 48-well plates with 200 µl of fibronectin and collagen hydrogel. Subject-matched ntMSCs and nbMSCs and unrelated abMSCs were utilized. Constructs were implanted subcutaneously in the dorsal region of NOD/SCID mice. Constructs were explanted 14 days after implantation for histological studies and CD31 immunohistochemistry (IHC) as previously described [29].

Microarray

Global gene expression from neonate-matched nbMSCs and ntMSCs was performed to gain further insight into the differences in their proangiogenic abilities. Total RNA was isolated from MSCs grown under standard conditions and then labeled and hybridized to Human Gene ST 2.1 human cDNA microarrays (Affymetrix, Santa Clara, CA, USA). Five biological replicates

(individual neonates) were analyzed by the University of Michigan Microarray Core. Human Gene ST 2.1 human cDNA microarrays (Affymetrix) were used to compare ntMSCs and nbMSCs. Differentially expressed probesets were identified by a $\log_2$ fold change >1 and an adjusted p-value <0.05 (adjusted for multiple comparisons using false discovery rate). Differentially expressed genes were further analyzed for gene ontology term overrepresentation analysis using the BINGO plugin of Cytoscape [35] as well as functional annotation clustering using DAVID [36,37]. The data discussed in this publication have been deposited in NCBI's GeneExpression Omnibus [38] and are accessible through GEO Series accession number GSE142563 (https://www.ncbi.nlm.nih.gov/geo/query/acc.cgi?acc=GSE142563).

Western Blotting

Protein was isolated from MSCs cultured under standard conditions and then quantified by bicinchoninic acid (BCA) assay (Pierce, Rockford, IL, USA). Next, 25 µg of total protein was loaded onto SDS-polyacrylamide gel electrophoresis and transferred to nitrocellulose membranes. Membranes were blocked in 5% skimmed milk for 1 hour at room temperature and then incubated with primary antibody (antibodies against SLIT3, Abcam, ab78365, Cambridge, UK) overnight at 4 °C. Goat anti-rabbit IgG (H+L) 800 CW was applied for 1 hour at room temperature (1:5000, LI-COR Biosciences, Lincoln, NE). Visualization and quantification were carried out with the LI-COR Odyssey® scanner and software (LI-COR Biosciences).

Transgenic Mice.

Slit3$^{+/+}$ and *Slit3*$^{-/-}$ mice on a CD-1 background were obtained from Dr. Sean Mclean (University of North Carolina). *Robo1*$^{+/+}$ and *Robo1*$^{-/-}$ mice (CD-1 background) were obtained from Dr. Marc Tessier-Lavigne (Stanford University). Neonatal mice (n = 3-5 per genotype group) at postnatal day 8-10 were anesthetized with isoflurane, and the whole thymus was obtained for IHC studies for CD31, SLIT3, and ROBO1. Thymus tissue was fixed with 10% formalin and embedded in

paraffin using standard protocols. The paraffin blocks were sectioned at 5 µm thickness. For immunohistochemistry, the sections were deparaffinized with xylene and rehydrated through a graded ethanol series of solutions. The sections were then subjected to heat-induced antigen retrieval in citrate buffer (pH 6.0), blocked with 5% BSA PBS buffer and incubated with primary antibodies at 4°C overnight. Anti-SLIT3 (1:100, Sigma-Aldrich, SAB2104337, St. Louis, MO), anti-ROBO1 (1:100, ab7279, Abcam, Cambridge, UK), and anti-CD31 (1:40, Novus Biologicals, Littleton, CO, USA) antibodies were used. The appropriate secondary antibody Alexa Fluor® (ThermoFisher Scientific) were used at a dilution of 1:200. Hoechst was used for nuclear counterstaining and all sections were mounted in Prolong Diamond Antifade Mountant (ThermoFisher Scientific). Images were obtained by confocal microscopy (Nikon A1Si, Melville, NY, USA).

In a separate experiment, the thymus was removed from *Slit3*$^{+/+}$ and *Slit3*$^{-/-}$ neonatal mice (n = 8 per genotype group) and mechanically minced into 1- 2 mm pieces. Explant culture was then performed as described for the isolation of human ntMSCs [29]. After 7 to 10 days, tissue fragments were removed, and migrated MSCs from tissue fragments were cultured until they reached 80% confluence.

Statistical Analysis

Statistical analysis was performed using a ratio t test of paired data or unpaired two-tailed Student's t-test using GraphPad Prism 9 (GraphPad Software, La Jolla, CA) when appropriate, and $p<0.05$ was considered significant. Data are presented as mean ± SD.

RESULTS

Neonatal thymus and bone MSCs possess unique pericytic signatures

We previously determined that human ntMSCs and nbMSCs could undergo *in vitro* multilineage differentiation and shared many surface markers expressed by abMSCs [28,29]. To further characterize these neonatal MSCs, we determined the expression of surface markers that have been previously associated with perivascular cells [39]. With flow cytometry, we observed that ntMSCs expressed higher levels of CD140b (PDGFRβ), lower levels of CD146 (MCAM/MUC18), equivalently low levels of CD140a (PDGFRα), and equivalently high levels of CD90 (Thy1) as compared to subject-matched nbMSCs (Fig. 1A and Supplementary Table S2). Furthermore, as compared to abMSCs and subject-matched nbMSCs, ntMSCs possessed a significantly higher transcript level of *TBX18* (Fig. 1B), which encodes for a transcription factor that is expressed in the perivascular cells of many organs in mice [8]. These results demonstrate that MSCs possess a tissue-specific pericytic phenotype.

Neonatal thymus MSCs are more proangiogenic than subject-matched nbMSCs.

After identifying that ntMSCs and nbMSCs possessed different pericytic signatures, we next assessed if ntMSCs would be functionally different than subject-matched nbMSCs in promoting neovascularization *in vitro* and *in vivo*. Since the primary mechanism by which MSCs stimulate angiogenesis is thought to be via the secretion of proangiogenic factors [40,41], we first determined if the secretome from these two types of MSCs would vary in their ability to promote HUVEC tube formation *in vitro*. HUVECs in Matrigel were exposed to conditioned medium obtained from ntMSC and nbMSC cultures. HUVEC tube and network formation were significantly increased in the group exposed to conditioned medium from ntMSCs as compared to that obtained from matched nbMSCs, as well as from cultures of unrelated abMSCs (Figs. 2A and 2B). We then observed that ntMSCs possessed increased transcript levels of the proangiogenic factors *VEGFA*, *FGF2*, *ANGPT1*, and *HIF1A* (Fig. 2C). The expression of *CXCL12* and *HGF*, both of which have been shown to encode factors involved in bone marrow-derived MSC mediated

angiogenesis [42,43], were similar to subject-matched nbMSCs (Fig. 2C). These results suggest that the secretome of ntMSCs is more proangiogenic than that of bone-derived MSCs.

Next, we determined the ability of ntMSCs and nbMSCs to promote angiogenesis in vivo by encapsulating them in a collagen-fibronectin plug along with HUVECs and then implanting them subcutaneously in NOD-SCID mice. Plugs were explanted after two weeks and were assessed for the presence of human CD31+ luminal structures containing red blood cells. We found that ntMSCs and HUVECs generated more perfused human CD31+ blood vessels as compared to nbMSCs and HUVECs (Figs. 2D and 2E). When compared to abMSCs, we also found that ntMSCs stimulated angiogenesis to a greater degree in vivo (Supplementary Figs. S1A and S1B). Collectively, these results indicate that MSCs isolated from the human neonatal thymus gland are more efficient in promoting angiogenesis *in vitro* and *in vivo* as compared to bone-derived MSCs.

Neonatal thymus MSCs are more motile and invasive than nbMSCs *in vitro*.

Perivascular cells such as MSCs are recruited and extend from adjacent areas to neovessels or capillaries that lack perivascular coverage [44,45], indicating that MSCs must be motile and be able to negotiate the extracellular matrix (ECM) to reach its appropriate destination. Further, MSCs must be motile and tissue invasive in order to home to areas of injury to impart their therapeutic effects [16].

Using a Boyden chamber assay, we first observed that ntMSCs had increased motility as compared to subject-matched nbMSCs (Fig. 3A). Next, we determined the ability of ntMSCs and nbMSCs to invade and migrate through fibrin, a key component of the early provisional matrix that is important for tissue repair [46]. We used a spheroid invasion assay [29,47] and determined that ntMSCs invaded fibrin more rapidly than nbMSCs (Figs. 3B and 3C). Altogether, this pairwise

comparison indicates that ntMSCs are consistently more motile and invasive than subject-matched nbMSCs.

Neonatal thymus MSCs have increased expression of SLIT3.

To further understand the mechanisms underlying the functional differences between ntMSCs and nbMSCs, we performed genome-wide profiling with microarray in pairs of MSCs isolated from 5 neonatal subjects. We found 116 genes that were at least 2x fold upregulated and 105 genes that were downregulated in ntMSCs as compared to nbMSCs (Fig. 4A, Supplementary Tables S3 and S4). Gene ontology category overrepresentation analysis revealed many processes related to tissue development in ntMSCs (Fig. 4B). Although functional annotation clustering did not identify any clusters related to angiogenesis, it did identify a cluster of genes (Annotation Cluster 5) enriched in ntMSCs that were related to axon guidance and Roundabout signaling (Supplementary Table S5), processes that have also been shown to regulate angiogenic sprouting [48,49]. Specifically, the secreted axon guidance molecule SLIT3 [50], also known to a proangiogenic factor [18,19], was found to be more highly expressed in ntMSCs (Supplementary Table S3), which we confirmed with qPCR and Western Blotting (Figs. 4C-E). Indeed, neutralizing SLIT3 in ntMSC conditioned medium with a specific antibody resulted in decreased HUVEC network formation in vitro, indicating that SLIT3 contributes to the paracrine effects of ntMSCs (Fig. 4F and Fig. S2).

SLIT3 is important for neonatal thymus vascularity

Global deficiency of SLIT3 causes congenital diaphragmatic hernia in mice that is due to a defect diaphragmatic angiogenesis, however the impact of SLIT3 on the vascular beds of other tissues is unknown [18]. We first investigated the spatial expression of SLIT3 in murine neonatal thymus

tissue since we had established that it was highly expressed in human ntMSCs. We found that SLIT3 is most dominantly in the peri-arteriolar region as well as within the stroma of the thymic cortex (Fig. 5A). Given the role of perivascular MSCs in thymus angiogenesis [51] and localization of SLIT3 expression to the perivascular cells in the neonatal thymus (Fig. 5A), we next postulated that SLIT3 played a role in thymus vascularization. To investigated this, we determined the CD31+ vascular density of thymus glands obtained from neonatal *Slit3*$^{+/+}$ and *Slit3*$^{-/-}$ mice. We found that vascular density was significantly decreased in thymus tissue from *Slit3* null mice (Figs. 5B and 5C). Altogether, these results confirm that SLIT3 is highly expressed in perivascular cells within the neonatal thymus gland and is important for thymus angiogenesis.

SLIT3 promotes the motile and invasive behavior of ntMSCs via ROBO1.

Given its ability to regulate the motility of various cell types [18,52-54], we investigated if SLIT3 could influence ntMSC invasive behavior in an autocrine fashion. We first determined the effects of rhSLIT3 on ntMSC and nbMSC spheroids and found that it increased invasion in fibrin gel but as a collective migration from the central mass of the spheroid and not as individual sprouts (Fig. 6A). We next isolated ntMSCs from *Slit3*$^{-/-}$ mice and found that they demonstrated blunted invasive behavior as compared to ntMSCs from *Slit3*$^{+/+}$ mice (Fig. 6B). Given the possibility that SLIT3 deficiency may have interfered with the development (and subsequent ability to migrate and invade) of the ntMSCs from these global kockout mice, we targeted *SLIT3* transcription in human ntMSCs with siRNA and found that decreasing SLIT3 expression also resulted in decreased length and number of sprouts from ntMSC spheroids, indicating that SLIT3 can directly regulate postnatal MSC motility and invasion in an autocrine fashion (Fig. 6C).

Given that ROBO1 and ROBO4 are potential receptors for the SLIT3 ligand [18], we first evaluated the transcript expression of the genes for both of these receptors in human MSCs (Fig. 6D). We

discovered that *ROBO1* transcript levels were up to 20-80 times more abundant than that of *ROBO4* transcripts in human MSCs (Fig. 6D). In the MSC pairs that we isolated from three patients, we found that ntMSCs had a higher ROBO1 transcript levels as compared to nbMSCs, but this was not significant (Fig. 6E). These results implied that ROBO1 (and not ROBO4) is likely the dominant receptor for SLIT3 in MSCs. To further confirm this, we targeted *ROBO1* transcription with specific siRNA and determined the effects on human ntMSC spheroid invasive sprouting. We found that targeting *ROBO1* transcription resulted in significantly decreased invasive ntMSC behavior (Fig. 6F). Altogether, these results demonstrate that SLIT3 promotes ntMSC invasion and motility in fibrin in an autocrine fashion via ROBO1.

ROBO1 participates in neonatal thymus angiogenesis.

The above findings indicated that MSCs can promote thymus angiogenesis via SLIT3 and that SLIT3 can act in an autocrine fashion to stimulate MSC motility and invasion. However, it is unclear how important MSC motility is to in vivo angiogenesis since sprouting is primarily formed by tip ECs [55]. To determine the presence of any relationship between ROBO1-mediated MSC motility and invasion and MSC-facilitated in vivo angiogenesis, we evaluated the vascularity of thymus glands from neonatal *Robo1*$^{+/+}$ and *Robo1*$^{-/-}$ mice. In wild-type mice, ROBO1 was found to be localized to the perivascular region of larger vessels, but not in the endothelium (Fig. 7A). ROBO1 deficiency resulted in a significantly decreased CD31+ blood vessel density within the cortex of the neonatal thymus gland (Fig. 7B and 7C), phenocopying the observations made in the thymus glands of *Slit3*$^{-/-}$ neonatal mice. Altogether, these results indicate that ROBO1 is important for neonatal thymus angiogenesis, in part by possibly mediating the autocrine effects of SLIT3 on ntMSC motility and invasion.

DISCUSSION

MSCs are currently being investigated in about 500 clinical trials for a variety of diseases [56]. The therapeutic activity of MSCs is thought to be in part due to its ability to secrete beneficial factors that promote survival, rejuvenation, and regeneration of diseased or stressed parenchymal cells [57]. A universal effect of exogenously transplanted MSCs is its ability to stimulate angiogenesis in the surrounding parenchyma, which may also contribute to the therapeutic effects of MSCs, especially in the setting of ischemia [58,59]. MSCs from a variety of tissues are being investigated as therapeutic agents, and our findings indicate that tissue source may be an important factor in determining their potency.

Our results of subject-matched MSCs also reveal that the secreted axon guidance molecule SLIT3 contributes to the proangiogenic effects of ntMSCs and that increased expression of *SLIT3* may partly explain why these MSCs were consistently found to be more potent at promoting angiogenesis as compared to subject-matched nbMSCs. These findings are consistent with the results of a prior study based on a comparison of bone marrow-derived MSC lines from two different individuals, and the MSC line that had a higher expression of *SLIT3* was more proangiogenic [19]. SLIT3 is known to act in a paracrine fashion to stimulate ECs and sprouting angiogenesis [18]. Interestingly, our studies indicate that SLIT3 may also act in an autocrine fashion via ROBO1 to stimulate MSC invasion and motility. Therefore *SLIT3* expression in MSCs may be a surrogate of their therapeutic potency, as it can stimulate both angiogenesis and MSC homing. Furthermore, our transcriptome analysis suggests that the tissue-specific properties of ntSMCs may extend beyond a difference in proangiogenic qualities as ntMSCs may have tendencies towards tissue development, formation, and regeneration.

The thymus gland is a highly vascular organ that can regenerate after injury and stress, and a marked angiogenic response mediated by MSCs supports thymus regeneration [51,62]. Further, a distinguishing characteristic of the thymus is that the entire vasculature, from the artery to

microvascular bed to vein, is completely invested by pericytes [31]. On the other hand, the vasculature and blood vascular sinusoids of the bone marrow have incomplete pericyte coverage, as with the vasculature from many other organs and tissues [30,32]. Our results suggest that ROBO1-mediated effects on MSCs, such as invasion and motility, are also important for thymus vascularization, indicating that SLIT3 exerts an autocrine effect on MSCs (Figs. 6A and 6B) that is independent of its paracrine effects on ECs that is mediated via ROBO4 [18]. MSC and pericyte motility are needed for neoangiogenesis as these cells are recruited from adjacent blood vessels to stabilize neovessels in a PDGFβ–dependent fashion [63]. Therefore a defect in SLIT3-ROBO1 signaling may result in defective MSC recruitment to neovasculature, leading to decreased stability of neovasculature, ultimately leading to decreased vascular density, similar to what is seen in EC-specific PDGFβ deficient mice [63]. Although SLIT3 and ROBO1 expression are generally found in the perivascular region, future studies will need to directly investigate the contribution of the SLIT3-ROBO1 signaling activity in perivascular MSCs on thymus angiogenesis and development by specific targeting using conditional knockout mouse models.

Portions of the thymus gland are routinely removed during neonatal and infant cardiac surgery, and thus this tissue presents as an ample and untapped source of neonatal MSCs, which we have previously shown to have therapeutic effects [29,59-61]. The results of this study further support the ntMSC as an attractive candidate for cell therapy given their superior proangiogenic properties. Patients with congenital heart disease who undergo cardiac surgery in the neonatal or early infancy periods are at risk of developing medical conditions secondary to defective perfusion or angiogenesis, such as capillary rarefaction from ventricular pressure overload which can contribute to heart failure [64-66], cerebral damage from complications of cardiopulmonary bypass and cardiac surgery [67,68], and myocardial ischemia and eventual heart failure from coronary obstruction after surgery [69]. Conceivably, autologous MSCs can be isolated from

discarded thymus tissue obtained during neonatal or infant cardiac surgery, expanded and cryopreserved *in vitro*, and then thawed and utilized when medically indicated.

In conclusion, our results have important implications for the translational efforts of MSCs into clinical therapy. MSC proangiogenic characteristics are tissue source-dependent and are related to the activity of an autocrine SLIT3-ROBO1 signaling axis. Neonatal thymus MSCs, which have high endogenous SLIT3-ROBO1 activity and proangiogenic behavior, warrants further evaluation as therapy for ischemic disease.

REFERENCES

1 Gupta PK, Chullikana A, Parakh R et al. A double blind randomized placebo controlled phase I/II study assessing the safety and efficacy of allogeneic bone marrow derived mesenchymal stem cell in critical limb ischemia [in English]. J Transl Med 2013;11.

2 Bura A, Planat-Benard V, Bourin P et al. Phase I trial: the use of autologous cultured adipose-derived stroma/stem cells to treat patients with non-revascularizable critical limb ischemia [in English]. Cytotherapy 2014;16(2):245-257.

3 Das AK, Bin Abdullah BJJ, Dhillon SS et al. Intra-arterial Allogeneic Mesenchymal Stem Cells for Critical Limb Ischemia are Safe and Efficacious: Report of a Phase I Study [in English]. World J Surg 2013;37(4):915-922.

4 Guhathakurta S, Subramanyan UR, Balasundari R et al. Stem cell experiments and initial clinical trial of cellular cardiomyoplasty. Asian Cardiovasc Thorac Ann 2009;17(6):581-586.

5 Heldman AW, DiFede DL, Fishman JE et al. Transendocardial mesenchymal stem cells and mononuclear bone marrow cells for ischemic cardiomyopathy: the TAC-HFT randomized trial. JAMA 2014;311(1):62-73.

6 Perin EC, Murphy MP, March KL et al. Evaluation of Cell Therapy on Exercise Performance and Limb Perfusion in Peripheral Artery Disease: The CCTRN PACE Trial (Patients With Intermittent Claudication Injected With ALDH Bright Cells). Circulation 2017;135(15):1417-1428.

7 Rigato M, Monami M, Fadini GP. Autologous Cell Therapy for Peripheral Arterial Disease: Systematic Review and Meta-Analysis of Randomized, Nonrandomized, and Noncontrolled Studies. Circ Res 2017;120(8):1326-1340.

8 Guimaraes-Camboa N, Cattaneo P, Sun Y et al. Pericytes of Multiple Organs Do Not Behave as Mesenchymal Stem Cells In Vivo. Cell Stem Cell 2017;20(3):345-359 e345.

9 Rafii S, Butler JM, Ding BS. Angiocrine functions of organ-specific endothelial cells. Nature 2016;529(7586):316-325.

10 Nolan DJ, Ginsberg M, Israely E et al. Molecular signatures of tissue-specific microvascular endothelial cell heterogeneity in organ maintenance and regeneration. Dev Cell 2013;26(2):204-219.

11 Chapel A, Bertho JM, Bensidhoum M et al. Mesenchymal stem cells home to injured tissues when co-infused with hematopoietic cells to treat a radiation-induced multi-organ failure syndrome. J Gene Med 2003;5(12):1028-1038.

12 Bronckaers A, Hilkens P, Martens W et al. Mesenchymal stem/stromal cells as a pharmacological and therapeutic approach to accelerate angiogenesis. Pharmacol Ther 2014;143(2):181-196.

13 Le Blanc K, Mougiakakos D. Multipotent mesenchymal stromal cells and the innate immune system. Nat Rev Immunol 2012;12(5):383-396.

14 Caplan AI. Why are MSCs therapeutic? New data: new insight. J Pathol 2009;217(2):318-324.

15 Karp JM, Teol GSL. Mesenchymal Stem Cell Homing: The Devil Is in the Details [in English]. Cell Stem Cell 2009;4(3):206-216.

16 Ullah M, Liu DD, Thakor AS. Mesenchymal Stromal Cell Homing: Mechanisms and Strategies for Improvement. iScience 2019;15:421-438.

17 Lu C, Li XY, Hu Y et al. MT1-MMP controls human mesenchymal stem cell trafficking and differentiation. Blood 2010;115(2):221-229.

18 Zhang B, Dietrich UM, Geng JG et al. Repulsive axon guidance molecule Slit3 is a novel angiogenic factor [in English]. Blood 2009;114(19):4300-4309.

19 Paul JD, Coulombe KLK, Toth PT et al. SLIT3-ROBO4 activation promotes vascular network formation in human engineered tissue and angiogenesis in vivo [in English]. J Mol Cell Cardiol 2013;64:124-131.

20 Crisan M, Corselli M, Chen WC et al. Perivascular cells for regenerative medicine. J Cell Mol Med 2012;16(12):2851-2860.
21 Efimenko A, Dzhoyashvili N, Kalinina N et al. Adipose-Derived Mesenchymal Stromal Cells From Aged Patients With Coronary Artery Disease Keep Mesenchymal Stromal Cell Properties but Exhibit Characteristics of Aging and Have Impaired Angiogenic Potential [in English]. Stem Cell Transl Med 2014;3(1):32-41.
22 Efimenko AY, Kochegura TN, Akopyan ZA et al. Autologous Stem Cell Therapy: How Aging and Chronic Diseases Affect Stem and Progenitor Cells [in English]. Bioresearch Open Acc 2015;4(1):26-38.
23 Choudhery MS, Khan M, Mahmood R et al. Bone marrow derived mesenchymal stem cells from aged mice have reduced wound healing, angiogenesis, proliferation and anti-apoptosis capabilities [in English]. Cell Biology International 2012;36(8):747-753.
24 Khan M, Mohsin S, Khan SN et al. Repair of senescent myocardium by mesenchymal stem cells is dependent on the age of donor mice [in English]. J Cell Mol Med 2011;15(7):1515-1527.
25 Rasmussen JG, Frobert O, Holst-Hansen C et al. Comparison of human adipose-derived stem cells and bone marrow-derived stem cells in a myocardial infarction model. Cell Transplant 2014;23(2):195-206.
26 Fijany A, Sayadi LR, Khoshab N et al. Mesenchymal stem cell dysfunction in diabetes. Mol Biol Rep 2019;46(1):1459-1475.
27 Paladino FV, Peixoto-Cruz JS, Santacruz-Perez C et al. Comparison between isolation protocols highlights intrinsic variability of human umbilical cord mesenchymal cells. Cell Tissue Bank 2016;17(1):123-136.
28 Wang S, Mundada L, Colomb E et al. Mesenchymal Stem/Stromal Cells from Discarded Neonatal Sternal Tissue: In Vitro Characterization and Angiogenic Properties. Stem Cells Int 2016;2016:5098747.
29 Wang S, Mundada L, Johnson S et al. Characterization and angiogenic potential of human neonatal and infant thymus mesenchymal stromal cells. Stem Cells Transl Med 2015;4(4):339-350.
30 Armulik A, Abramsson A, Betsholtz C. Endothelial/pericyte interactions. Circ Res 2005;97(6):512-523.
31 Muller SM, Stolt CC, Terszowski G et al. Neural crest origin of perivascular mesenchyme in the adult thymus. J Immunol 2008;180(8):5344-5351.
32 Zetterberg E, Vannucchi AM, Migliaccio AR et al. Pericyte coverage of abnormal blood vessels in myelofibrotic bone marrows. Haematologica 2007;92(5):597-604.
33 Foster K, Sheridan J, Veiga-Fernandes H et al. Contribution of neural crest-derived cells in the embryonic and adult thymus. J Immunol 2008;180(5):3183-3189.
34 Sheng G. The developmental basis of mesenchymal stem/stromal cells (MSCs). BMC Dev Biol 2015;15:44.
35 Maere S, Heymans K, Kuiper M. BiNGO: a Cytoscape plugin to assess overrepresentation of gene ontology categories in biological networks. Bioinformatics 2005;21(16):3448-3449.
36 Huang da W, Sherman BT, Lempicki RA. Systematic and integrative analysis of large gene lists using DAVID bioinformatics resources. Nat Protoc 2009;4(1):44-57.
37 Huang da W, Sherman BT, Lempicki RA. Bioinformatics enrichment tools: paths toward the comprehensive functional analysis of large gene lists. Nucleic Acids Res 2009;37(1):1-13.
38 Edgar R, Domrachev M, Lash AE. Gene Expression Omnibus: NCBI gene expression and hybridization array data repository. Nucleic Acids Res 2002;30(1):207-210.
39 Ferland-McCollough D, Slater S, Richard J et al. Pericytes, an overlooked player in vascular pathobiology. Pharmacol Ther 2017;171:30-42.
40 Kwon HM, Hur SM, Park KY et al. Multiple paracrine factors secreted by mesenchymal stem cells contribute to angiogenesis. Vascul Pharmacol 2014;63(1):19-28.

41 Kuchroo P, Dave V, Vijayan A et al. Paracrine factors secreted by umbilical cord-derived mesenchymal stem cells induce angiogenesis in vitro by a VEGF-independent pathway. Stem Cells Dev 2015;24(4):437-450.
42 Zhang L, Zhou Y, Sun X et al. CXCL12 overexpression promotes the angiogenesis potential of periodontal ligament stem cells. Sci Rep 2017;7(1):10286.
43 Crisostomo PR, Wang Y, Markel TA et al. Human mesenchymal stem cells stimulated by TNF-alpha, LPS, or hypoxia produce growth factors by an NF kappa B- but not JNK-dependent mechanism. Am J Physiol Cell Physiol 2008;294(3):C675-682.
44 Jain RK. Molecular regulation of vessel maturation. Nat Med 2003;9(6):685-693.
45 Berthiaume AA, Grant RI, McDowell KP et al. Dynamic Remodeling of Pericytes In Vivo Maintains Capillary Coverage in the Adult Mouse Brain. Cell Rep 2018;22(1):8-16.
46 Barker TH, Engler AJ. The provisional matrix: setting the stage for tissue repair outcomes. Matrix Biol 2017;60-61:1-4.
47 De Wever O, Hendrix A, De Boeck A et al. Single cell and spheroid collagen type I invasion assay. Methods Mol Biol 2014;1070:13-35.
48 Adams RH, Eichmann A. Axon guidance molecules in vascular patterning. Cold Spring Harb Perspect Biol 2010;2(5):a001875.
49 Larrivee B, Freitas C, Suchting S et al. Guidance of vascular development: lessons from the nervous system. Circ Res 2009;104(4):428-441.
50 Brose K, Bland KS, Wang KH et al. Slit proteins bind Robo receptors and have an evolutionarily conserved role in repulsive axon guidance. Cell 1999;96(6):795-806.
51 Lax S, Ross EA, White A et al. CD248 expression on mesenchymal stromal cells is required for post-natal and infection-dependent thymus remodelling and regeneration. FEBS Open Bio 2012;2:187-190.
52 Tanno T, Fujiwara A, Sakaguchi K et al. Slit3 regulates cell motility through Rac/Cdc42 activation in lipopolysaccharide-stimulated macrophages. FEBS Lett 2007;581(5):1022-1026.
53 Zhang C, Guo H, Li B et al. Effects of Slit3 silencing on the invasive ability of lung carcinoma A549 cells. Oncol Rep 2015;34(2):952-960.
54 Schubert T, Denk AE, Ruedel A et al. Fragments of SLIT3 inhibit cellular migration. Int J Mol Med 2012;30(5):1133-1137.
55 Gerhardt H, Golding M, Fruttiger M et al. VEGF guides angiogenic sprouting utilizing endothelial tip cell filopodia. J Cell Biol 2003;161(6):1163-1177.
56 Squillaro T, Peluso G, Galderisi U. Clinical Trials With Mesenchymal Stem Cells: An Update. Cell Transplant 2016;25(5):829-848.
57 Fu Y, Karbaat L, Wu L et al. Trophic Effects of Mesenchymal Stem Cells in Tissue Regeneration. Tissue Eng Part B Rev 2017;23(6):515-528.
58 Tao HY, Han ZB, Han ZC et al. Proangiogenic Features of Mesenchymal Stem Cells and Their Therapeutic Applications [in English]. Stem Cells International 2016.
59 Wang S, Huang S, Gong L et al. Human Neonatal Thymus Mesenchymal Stem Cells Promote Neovascularization and Cardiac Regeneration. Stem Cells Int 2018;2018:8503468.
60 Sondergaard CS, Hodonsky CJ, Khait L et al. Human thymus mesenchymal stromal cells augment force production in self-organized cardiac tissue. Ann Thorac Surg 2010;90(3):796-803; discussion 803-794.
61 Chery J, Huang S, Gong L et al. Human Neonatal Thymus Mesenchymal Stem/Stromal Cells and Chronic Right Ventricle Pressure Overload. Bioengineering (Basel) 2019;6(1).
62 Park HJ, Kim MN, Kim JG et al. Up-regulation of VEGF expression by NGF that enhances reparative angiogenesis during thymic regeneration in adult rat [in English]. Bba-Mol Cell Res 2007;1773(9):1462-1472.

63 Lindblom P, Gerhardt H, Liebner S et al. Endothelial PDGF-B retention is required for proper investment of pericytes in the microvessel wall. Genes Dev 2003;17(15):1835-1840.
64 Friehs I, Moran AM, Stamm C et al. Promoting angiogenesis protects severely hypertrophied hearts from ischemic injury. Ann Thorac Surg 2004;77(6):2004-2010; discussion 2011.
65 Kitahori K, He H, Kawata M et al. Development of left ventricular diastolic dysfunction with preservation of ejection fraction during progression of infant right ventricular hypertrophy. Circ Heart Fail 2009;2(6):599-607.
66 Wehman B, Kaushal S. The emergence of stem cell therapy for patients with congenital heart disease. Circ Res 2015;116(4):566-569.
67 Maeda T, Sarkislali K, Leonetti C et al. Impact of Mesenchymal Stromal Cell Delivery Through Cardiopulmonary Bypass on Postnatal Neurogenesis. Ann Thorac Surg 2019.
68 Beca J, Gunn JK, Coleman L et al. New white matter brain injury after infant heart surgery is associated with diagnostic group and the use of circulatory arrest. Circulation 2013;127(9):971-979.
69 Goldsmith MP, Allan CK, Callahan R et al. Acute coronary artery obstruction following surgical repair of congenital heart disease. J Thorac Cardiovasc Surg 2019.

FIGURE TITLES AND LEGENDS

Figure 1. Pericytic signature of human neonate-matched MSCs.

A, Neonatal thymus MSCs possessed a surface marker expression as determined by flow cytometry that was more pericyte-like as compared to nbMSCs (also see Table S1, n=3 subjects). B, Transcript expression of perivascular cell-associated factor *TBX18* in subject-matched ntMSCs and nbMSCs as determined by qPCR. Each data pair represents ntMSCs and nbMSCs that were isolated from a single patient and all data compared with a ratio t test.

Figure 2. Neonatal thymus MSCs are more proangiogenic than subject-matched nbMSCs.

A, Conditioned medium (CM) from ntMSCs promoted greater HUVEC network formation as conditioned medium from nbMSCs and abMSCs. Scale bar = 200 μm. B, Quantification of HUVEC network formation in A. Each data point represents a randomly selected field of analysis. (Results are from n=3 subjects). C, Neonatal thymus MSCs had greater transcript levels of *ANGPT1* and *HIF1A* as compared to matched nbMSCs. Each data pair represents ntMSCs and nbMSCs that were isolated from a single patient and all data compared with a ratio t test. D, CD31 immunohistochemistry of MSC/HUVEC-seeded collagen/fibronectin constructs implanted in NOD

SCID mice for 14 days. Scale bars = 50 μm. E, Quantification of CD31 vascular density of constructs in D, showing that ntMSCs stimulated more angiogenesis in vivo (n=5 animals with two constructs per animal; ntMSCs and nbMSCs isolated from the same subject). Each data point represents a randomly selected field of analysis.

Figure 3. Neonatal thymus MSCs are more invasive and motile than bone MSCs.

A, Quantification of Boyden chamber assay results for subject-matched ntMSCs and nbMSCs (n=3 subjects). Each data point represents the average of four technical replicates for each cell line and averaged data points were compared with a ratio t test. B, Spheroid comprised of ntMSCs manifested more sprouting/invasion in fibrin as compared to those made with matched nbMSCs. Scale bars = 100 μm. C, Quantification of number and length of branches from spheroids in B (n=3 subjects) with each data point representing analysis from a single, independent spheroid.

Figure 4. SLIT3 is upregulated in ntMSCs and is important for their proangiogenic paracrine effects. A, Heatmap of differentially expressed genes in subject-matched ntMSCs and nbMSCs as determined by microarray (also see Supplementary Tables S3 and S4, n=5 subjects). B, Network of gene ontology overrepresentation analysis of overexpressed genes in ntMSCs (Supplementary Table S3) indicate enrichment for development and morphogenesis processes. C, *SLIT3* transcript expression in subject-matched ntMSCs and nbMSCs as determined by qPCR. Each data pair represents ntMSCs and nbMSCs that were isolated from a single patient. D and E, SLIT3 expression in subject-matched ntMSCs and nbMSCs as determined by Western blotting with quantification (results are representative of n=2 subjects). F, Neutralizing SLIT3 in the conditioned medium (CM) obtained from ntMSCs decreases their ability to promote HUVEC network formation in vitro. Experiments were performed wtih conditioned medium generated from three different ntMSC lines. Three random fields were analyzed per group, averaged, and then compared with a Student's t test.

Figure 5. SLIT3 is important for neonatal thymus angiogenesis. A, Immunohistochemistry of wildtype *Slit3*$^{+/+}$ mouse neonatal thymus gland showing localization of SLIT3 to the perivascular region of arterioles (results representative of samples from n=3 animals). Scale bars = 50 μm. B and C, CD31 immunohistochemistry of thymus glands from *Slit3*$^{+/+}$ and *Slit3*$^{-/-}$ neonatal mice with quantification of CD31 vascular density (n=5 thymus glands per group). Each data point represents a randomly selected field of analysis. Scale bars= 60 μm.

Figure 6. ROBO1 mediates SLIT3 invasive motile effects on ntMSCs. A, Recombinant human SLIT3 promotes a general spreading of ntMSC spheroids in fibrin gel. B, ntMSCs from *Slit3*$^{-/-}$ neonatal mice have decreased invasive motile activity than ntMSCs from *Slit3*$^{+/+}$ neonatal mice. ntMSCs were pooled from n=8 animals/genotype group. C, Targeting *SLIT3* transcription with siRNA inhibits ntMSC spheroid invasive sprouting. D, *ROBO1* is expressed 20-80 times more than *ROBO4* in MSCs. Each data pair represents ntMSCs and nbMSCs that were isolated from a single patient and data were compared with a ratio t test. E, *ROBO1* transcript levels in paired human nbMSCs and ntMSCs as determined by qPCR and data were compared with a ratio t test. Each data pair represents ntMSCs and nbMSCs that were isolated from a single patient. F, Targeting *ROBO1* transcription with siRNA inhibits ntMSC spheroid invasive sprouting. Spheroid experiment results (A, C, and F) are representative of at least four independent experiments utilizing MSCs isolated from n=4 subjects. Data points for qPCR of siRNA treated MSCs represent technical replicates and data points for spheroid branching analysis represent a single spheroid. Spheroid experimental results were analyzed with a Student's t test. Scale bars = 100 μm.

Figure 7. ROBO1 participates in neonatal thymus angiogenesis. A, Immunohistochemistry of wildtype *Robo1*$^{+/+}$ mouse neonatal thymus gland showing localization of ROBO1 to the perivascular region of arterioles (Results representative tissue from n=3 animals). Scale bars = 10 μm. B and C, CD31 immunohistochemistry of thymus glands from *Robo1*$^{+/+}$ and *Robo1*$^{-/-}$ neonatal mice with quantification of CD31 vascular density (At least n=5 sections were analyzed

from n=3 thymus glands per genotype group). Each data point represents a randomly selected field of analysis. Scale bars = 60 μm.

SUPPLEMENTARY FIGURES AND TABLES

Supplementary Figure S1. Neontatal thymus MSCs was superior to adult bone marrow-derived MSCs in promoting angiogenesis in vivo. A and B, CD31 immunohistochemistry of abMSC/HUVEC-seeded collagen/fibronectin (A) and ntMSC/HUVEC-seeded collagen/fibronectin (B) constructs implanted in NOD SCID mice for 14 days. Scale bars = 50 μm. Only 20% (1/5 constructs) of explanted constructs from the abMSC/HUVEC group demonstrated CD31 positive luminal structures whereas 100% of ntMSC/HUVEC constructs possessed numerous CD31 positive vessels (n=5 animals with two constructs per animal).

Supplementary Figure S2. Neutralizing SLIT3 in the conditioned medium (CM) obtained from ntMSCs decreases their ability to promote HUVEC network formation in vitro. A specific anti-SLIT3 antibody can decrease the ability of conditioned medium from ntMSCs to promote HUVEC network formation in vitro. Data from these experiments are quantified and analyzed in Fig. 4F.

Supplementary Table S1. qPCR primers used in this study.

Supplementary Table S2. Pericytic surface marker expression of three subject-matched neonatal thymus and bone MSCs as determined by flow cytometry.

Supplementary Table S3. Upregulated genes (> 2.0x fold) in ntMSCs as compared to subject-matched nbMSCs as determined by microarray analysis.

Supplementary Table S4. Down-regulated genes in ntMSCs as compared to subject-matched nbMSCs determined by microarray analysis.

Supplementary Table S5. Functional annotation analysis using DAVID of overexpressed genes in ntMSCs as identified by microarray.

Supplementary Table S6. Details of the cell lines and subjects.

Supplementary Table S7. Specific cell lines used in each experiment.

Supplementary Table S8. Individual data values and cell lines used for qPCR gene expression shown in Figs. 1B, 2C, 4C, 6D, and 6E.

4/5/2020

Dear Dr. Atala,

We thank the reviewers for their critical, detailed appraisal of our manuscript and their insightful suggestions. We have performed extensive revisions as suggested and have included new data and analyses. Overall the conclusions have not changed, but the manuscript is much stronger and we feel that it will be interesting for the audience of *Stem Cells Translational Medicine*.

Here are our specific responses to the Reviewers:

Reviewer 1

Comments:

1) **The authors should investigate the exact mechanism by which ROBO mediates angiogenesis and the molecular pathways involved.**

We appreciate the comment from the reviewer and we certainly share the reviewer's viewpoint. In this study we have identified the importance of SLIT3-ROBO1 signaling in angiogenesis, something that has never been described in detail. Current and future studies will focus on the molecular mechanisms in MSCs which mediate ROBO1's effects on this cell type.

2) **A thorough bioinformatics analysis should be performed related to differentially expressed genes between neonatal thymus MSCs and neonatal bone MSCs and additional experiments should be conducted for a more detailed functional analysis.**

With the assistance of our DNA microarray core facility and the use of the open-source bioinformatics software platform Cytoscape, we feel that we have performed a thorough bioinformatics analysis. Remarkably, a relatively small number of genes were differentially expressed (106 were more than two-fold upregulated in ntMSCs). The results of this microarray led us to focus on SLIT3, however we also share the reviewer's opinion that other factors may play an important role in the motile, invasive and proangiogenic behavior of ntMSCs and should be the topic of future investigations. The last sentence of the second paragraph on page 15 discusses this sentiment. Also, the microarray data has been deposited in the NCBI repository for other investigators to analyze and we hope that this stimulates additional lines of research.

3) **The authors also claim that their results have important implications for the translational efforts of MSCs into the clinical therapy. However, they shoud provide evidence and discuss in more detail the clinical importance and the potential use of the neonatal thymus MSCs. Questions like how can be this approach transferred to the clinic and what is the optimal number of cells for such therapeutic modalities are of high importance for the novelty of this study.**

We agree with the reviewer that we had neglected to expand on the translational implications further. We have done so in the second to the last paragraph of the Discussion section. Specifics of

optimal route of administration, cell dosing, and timing of therapy would need to be rigorously determined from multiple additional animal studies.

Minor comments

1) Molecular weight (MW) information should be included in western blot images.

We have included the MW.

2) Images of low quality.

We have now included high quality images with the resubmission.

Reviewer 2

1. **While the manuscript provided important mechanistic studies for the tissue-specific differences of MSCs in their proangiogenic and motility property, to better align with the scope of the journal SCTM, it needs to put more effort into highlighting the clinical relevance of their study.**

We thank the reviewer for pointing this out and have added a paragraph in the Discussion section that describes the translational implications of our results.

2. In the last sentence of the abstract, the author concluded that "ntMSCs possess increased proangiogenic and invasive behaviors which are in part mediated by the paracrine and autocrine effects of SLIT3." However, only the autocrine effect is supported by the study and discussed in the manuscript.

The paracrine behavior of SLIT3, i.e., the effects on endothelial cells, have been described in detail by prior studies and we have referenced them. But we also agree with the reviewer that we did not provide direct evidence that the paracrine proangiogenic effects of ntMSCs on ECs is in part mediated by SLIT3. Therefore, we have determined the importance of SLIT3 in the secretome of ntMSCs with a new conditioned medium experiment. The results of this new experiment are shown in Fig. 4F and Fig. S2 and described in the corresponding Results section and Figure Legends. We neutralized SLIT3 in the ntMSC conditioned medium with a specific antibody and determined the effects on HUVEC network formation in vitro. We found that blocking SLIT3 with the specific antibody significantly decreased the stimulatory effects of ntMSC conditioned medium on HUVEC network formation in vitro. These results indicate that SLIT3 does contribute to the proangiogenic paracrine effects of ntMSCs and furthers strengthens this study.

3. The number of subjects studied does not correlate with the dot plots in the figures. That might be caused by multiple images/samples that are analyzed for the same donor cells. However, for statistical analysis and presentation purposes, the mean for samples from the same donor should be shown instead of all the data points. Please make sure statistical analysis was performed with the claimed number of subjects rather than the number of data in the set.

The reviewer has astutely pointed out several critical mistakes (due to the figure legends not being updated as additional experiments were performed). We have performed the analysis as the reviewer

has suggested. We have also clarified in the legends of each figure as to what the data points represent in graphs and plots.

4. For Figure 2C, the author concluded that the transcript levels of VEGFA, FGF2, ANGPT1, and HIF1A are higher. However, there is donor to donor variations as in some donor cells, the transcript levels are decreased. The reader will be interested to know whether those showing lower transcript levels for different genes are all from the same donor. It will be more helpful if the author could show the transcript level by labeling individual donors (or show that in a table form).

We have analyzed the gene expression data as the reviewer suggested in point 3. In the new analysis of qPCR data, which impacts Fig. 1B, Fig. 2C, Fig. 4C, Fig. 6D, and Fig. 6E, *TBX18*, *ANGPT1*, *HIF1A*, and *SLIT3* are significantly different while the other genes are not. We have modified the corresponding Results section as well as Figure Legends to reflect this. We have also included Supplementary Table S6 which includes the cell lines that were used this study, Supplementary Table S7 which specifies which cell lines were used for each experiment, and Supplementary Table S8 which include the data for the qPCR experiments for each cell line. Importantly, the new analysis of the results do not change our overall conclusions.

5. Similarly to point 4, for the different experiments, a different number of subjects were used. This raises the question of which sets of experiments are from the same donor. It will be helpful to provide more information about the donors (a list of donor/patient) for each experiment performed.

Please see response to point 4.

6. In figure 6D, it is not clear why the ratio of ROBO1/ROBO4 is shown and what do the results that ROBO1/ROBO4 levels are higher in nbMSCs imply and relates to other results. ROBO4 is an endothelial-specific receptor for SLIT3; its levels in MSCs will be expected to be low.

We appreciate the comment and realize that the intent of this experiment and data was not clearly defined. We determined that SLIT3 promoted MSC invasive and motile behavior (Figs. 6A and 6B). Since ROBO1 and ROBO4 have been shown to bind the SLIT3 ligand (reference 18), we reasoned that either ROBO1 or ROBO4 (or both), could be mediating the autocrine effects of SLIT3 in MSCs. Therefore, to determine which ROBO receptor was mediating the autocrine effects, we ascertained the level of expression for both in MSCs, which is shown in Fig 6D (ROBO1 expression relative to ROBO4 in each MSC line evaluated). The reviewer is correct in mentioning that ROBO4 is considered an endothelial specific receptor however we wanted to be thorough in examining all possibilities. To clarify the ambiguities in our original submission, we have made several changes to the sentences in the Results section "SLIT3 promotes the motile and invasive behavior of ntMSCs via ROBO1."

7. Page 16 line 3, "SLIT3 exerts an autocrine…that is independent of its paracrine effects…" The data from the current study, which only showed a relative expression level of ROBO4 to ROBO1, is insufficient to support this conclusion.

We appreciate the comment and realize that the sentence was written ambiguously. The first part of the sentence mentions the autocrine effects of MSC mediated SLIT3 via the ROBO1 receptor. Figure 6 provides proof for this statement.The last part of the sentence that is concerning the paracrine effects of MSC mediated SLIT3 is concerning the endothelial cell as the target (via the EC-specific ROBO4 receptor). The effects of SLIT3 on ECs via ROBO4 has been documented by Zhang et al, which is cited.

We have also included a new experiment to neutralize SLIT3 in the MSC secretome as described in response to point #2 above. We have revised this sentence to make it more clear.

8. **The manuscript also has a few typos and formatting errors that need to be corrected.**

We have corrected these errors.

a. **Terms like in vitro and in vivo need to be italicized.**

We thank the reviewer for pointing out these errors and we have made these corrections.

b. **In the abstract and first paragraph, "pro-angiogenic and pro-regenerative" were used, whereas in other parts, "proangiogenic and proregenerative" were used.**

The spelling of the words needs to be consistent. We thank the reviewer for pointing out these inconsistencies and we have made these corrections.

c. **Page 4, line 32, "it is not know" should be "it is not known".**

We thank the reviewer for pointing out this error and we have made this correction.

d. **Page 24, line 8 and 10 "flow cytoemtry" should be "flow cytometry".**

We thank the reviewer for pointing out this error and we have made this correction.

In summary we again thank the reviewers for taking the time to critically read our manuscript and provide very useful suggestions. Please let me know if you have any questions.

Thanks,

Ming-Sing Si, MD